Mechanism of memantine block of NMDA-activated channels in rat retinal ganglion cells: uncompetitive antagonism

Huei-Sheng Vincent Chen and Stuart A. Lipton *

Laboratory of Cellular and Molecular Neuroscience, Children's Hospital and Program in Neuroscience, Harvard Medical School, Boston, MA 02115, USA

1. *N*-methyl-D-aspartic acid (NMDA)-activated currents were recorded from dissociated rat retinal ganglion cells using whole-cell recording. The NMDA open-channel blocking drug memantine was evaluated for non-competitive and/or uncompetitive components of antagonism. A rapid superfusion system was used to apply various drugs for kinetic analysis.

2. Dose–response data revealed that memantine blocked 200 μM NMDA-evoked responses with a 50% inhibition constant (IC_{50}) of ~1 μM at −60 mV and an empirical Hill coefficient of ~1. The antagonism followed a bimolecular reaction process. This 1:1 stoichiometry is supported by the fact that the macroscopic blocking rate of memantine (k_{on}) increased linearly with memantine concentration and the macroscopic unblocking rate (k_{off}) was independent of it. The estimated pseudo-first order rate constant for macroscopic blockade was 4×10^5 M^{-1} s^{-1} and the rate constant for unblocking was 0·44 s^{-1}. Both the blocking and unblocking actions of memantine were well fitted by a single exponential process.

3. The k_{on} for 2 μM memantine decreased with decreasing concentrations of NMDA. By analysing k_{on} behaviour, we estimate that memantine has minimal interaction with the closed-unliganded state of the channel. As channel open probability (P_o) approached zero, a small residual action of memantine may be explained by the presence of endogenous glutamate and glycine.

4. Memantine could be trapped within the NMDA-gated channel if it was suddenly closed by fast washout of agonist. The measured gating process of channel activation and deactivation appeared at least 10–20-fold faster than the kinetics of memantine action. By combining the agonist and voltage dependence of antagonism, a trapping scheme was established for further kinetic analysis.

5. With low agonist concentrations, NMDA-gated channels recovered slowly from memantine blockade. By analysing the probability of a channel remaining blocked, we found that memantine binding appeared to stabilize the open conformation of the blocked channel and did not affect ligand affinity. Validity of the 'trapping model' and stabilization of the open conformation were further suggested by agreement between the predicted dose–response curve for NMDA in the presence of 2 μM memantine and the empirically derived dose–response relationship.

6. Based on simple molecular schemes, the degree of blockade at various concentrations of agonist for 'pure' non-competitive *vs.* uncompetitive inhibition was computer simulated. The measured degree of blockade by 6 μM memantine was close to ideal for pure uncompetitive antagonism. Taken together, we conclude that the predominant mechanism of open-channel blockade by memantine is uncompetitive. In general, the relative magnitude of the dissociation rate of an open-channel blocker from the open but blocked channel (the apparent off-rate) compared with the rate of leaving the closed and blocker-trapped state (the leak rate) will determine the contribution of uncompetitive *vs.* non-competitive actions, respectively.

7. Millimolar internal Cs^+ competed with memantine for binding in the NMDA-gated channel, and reduced the association rate of memantine, but had no effect on the voltage dependence of the dissociation rate. After removal of Cs^+, the calculated K_I for memantine remained voltage dependent. These observations would be difficult to reconcile with models in which memantine binds to a site outside the channel pore and instead strongly support the supposition that the blocking site for memantine is within the permeation pathway.

* To whom correspondence should be addressed at the Children's Hospital.

Excessive levels of glutamate have been linked to neuronal cell death in hypoxic-ischaemic brain injury, epilepsy, trauma, and several degenerative neurological disorders such as Huntington's disease, Parkinson's disease, and HIV-1-associated cognitive/motor complex (AIDS dementia) (reviewed in Rothman & Olney, 1987; Choi, 1988; Meldrum & Garthwaite, 1990; Lipton & Rosenberg, 1994; Lipton & Gendelman, 1995). In many areas of the central nervous system (CNS) the predominant form of this neurotoxicity appears to be mediated by activation of the *N*-methyl-D-aspartate (NMDA) subtype of glutamate receptor and subsequent influx of excessive Ca^{2+}. Various types of NMDA receptor antagonists have therefore attracted much attention for their therapeutic potential against these diseases (reviewed in Wong & Kemp, 1991; Rogawski, 1993; Lipton, 1993; Lipton & Rosenberg, 1994). Among these different types of NMDA receptor antagonists, both the competitive NMDA binding site antagonists and glycine site antagonists, theoretically, will not be able to distinguish low levels of receptor activation by normal neurotransmission from excessive activation by toxic levels of glutamate due to the mandatory roles of NMDA and glycine in receptor activation (Lipton, 1993). Organic open-channel blockers of NMDA-gated receptors, e.g. dissociative anaesthetics, have therefore been investigated for their agonist- (or use-) and voltage-dependent nature of antagonism (MacDonald *et al.* 1991). However, the molecular mode of action of these NMDA open-channel blockers has not been clearly defined and has usually been characterized pharmacologically as 'non-competitive' and/or 'uncompetitive' blockade (e.g. see Kemp, Foster & Wong, 1987; Rogawski, 1993). In terms of molecular pharmacology, a non-competitive antagonist will bind to and unbind from a receptor irrespective of the presence of agonist; a pure uncompetitive antagonist will only bind to and leave a receptor which has been activated by agonist. Theoretically, a non-competitive antagonist will block receptors irrespective of the concentration of agonist, and only an uncompetitive antagonist will display a greater degree of blockade with greater activation of receptors by agonist (see theoretical equations in Pennefather & Quastel, 1982). However, the substantial lipophilicity of many open-channel blockers make pure uncompetitive antagonism impossible because these drugs can 'leak' out from the blocking site through a lipophilic pathway when the blocker is trapped in the unliganded and suddenly closed channel (Hille, 1984). Thus, virtually all open-channel blockers display characteristics in between those of a pure non-competitive and a pure uncompetitive antagonist. The therapeutic advantage of these agents lies in the uncompetitive component of open-channel blockade due to its inherent nature of increased inhibition with increasing concentrations of agonist (Chen *et al.* 1992; Lipton, 1993). Here, we use the drug memantine as an example to elucidate the molecular nature of antagonism against NMDA-operated receptors, to establish a stepwise method with molecular schemes to dissect the difference between non-competitive and uncompetitive modes of action, and to outline a molecular basis for evaluating therapeutic advantages among this class of open-channel blockers.

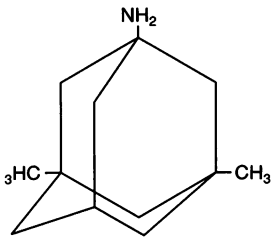

Structure of memantine

Memantine (1-amino-3,5-dimethyladamantane hydrochloride) is known to have anti-Parkinsonian (Schneider, Fischer, Clemens, Balzereit, Fünfgeld & Haase, 1984) and anti-epileptic (Meldrum, Turski, Schwarz, Czuczwar & Sontag, 1986) properties. It is an analogue of amantadine, an anti-A2 influenza agent (reviewed in Tominack & Hayden, 1987). Both adamantane derivatives have been used clinically for Parkinson's disease for many years in the USA or in Europe (Schwab, England, Poskanzer & Young, 1969; Schneider *et al.* 1984). Relatively recently, memantine was reported to block NMDA-evoked current in embryonic mouse spinal neurons (Bormann, 1989). We have previously shown that memantine, at low micromolar concentrations, was neuroprotective and inhibited NMDA-induced responses by a mechanism of open-channel block (Chen *et al.* 1992). The observations that support this blocking mechanism are as follows: (i) memantine blockade of NMDA-induced current is voltage and agonist dependent; (ii) the macroscopic unblocking time constant of memantine blockade is slower at hyperpolarized potentials and behaves as an exponential function of membrane potential over the range of −80 to +50 mV; (iii) memantine blockade is no longer observed after pre-exposure to 3 mM magnesium, a well defined open-channel blocker of NMDA receptor-operated channels (Nowak, Bregestovski, Ascher, Herbert & Prochiantz, 1984; Mayer, Westbrook & Guthrie, 1984); (iv) memantine blocks the NMDA-induced current to a greater degree at higher concentrations of agonist and displays an uncompetitive mode of antagonism; and (v) single-channel recordings show that the predominant effect of memantine is to decrease the frequency of channel opening, while slightly shortening the mean open time; memantine has no effect on the unitary channel conductance (Chen *et al.* 1992).

In the present study, we describe additional experiments to address the precise mode of action of memantine. We provide evidence that memantine binds to a site inside NMDA receptor-operated channels by a bimolecular reaction, that memantine has negligible interaction with the closed/unliganded channel, and that memantine can be trapped inside the channel when the channel is abruptly closed. Adapting a well-known method of kinetic analysis (Miller, Latorre & Reisin, 1987), we present a quantitative model for these data utilizing a trapping scheme. Finally, by using this scheme, we conclude that the relative magnitude of the dissociation rates from opened or trapped channels will

determine the magnitude of the uncompetitive or non-competitive components of antagonism of this type of open-channel blocker. In turn, we hypothesize that these components will determine the potential clinical safety and utility of these drugs in terms of the molecular pharmacology.

METHODS

Retinal ganglion cell culture

For retinal ganglion cell (RGC) fluorescent labelling, dissociation and culture, we used techniques that we have detailed elsewhere (Leifer, Lipton, Barnstable & Masland, 1984; Lipton & Tauck, 1987; Aizenman, Frosch & Lipton, 1988). Briefly, RGCs of 4-day-old Long–Evans rats were retrogradely labelled with the fluorescent dye Granular Blue by injection into the superior colliculus under anaesthesia as described by Lipton & Tauck (1987). Two to six days later, the animals were killed by cervical dislocation. Following enucleation, the retinas were dissociated with papain and plated onto glass cover slips coated with poly-L-lysine in 35 mm tissue culture dishes. The growth medium was comprised of Eagle's minimum essential medium supplemented with 0·7% (w/v) methylcellulose, 0·3% (w/v) glucose, 2 mM glutamine, 5% (v/v) rat serum and 1 μg ml^{-1} gentamicin. RGCs were identified by the presence of the dye Granular Blue. As an alternative method, a subpopulation of RGCs could be identified by their large size, oval shape and eccentric nucleus. No obvious differences in the characteristics of voltage-dependent or ligand-gated (including NMDA-gated) channels had been found previously by our laboratory when comparing different sizes of RGCs (Lipton & Tauck, 1987; Aizenman *et al.* 1988; Karschin, Aizenman & Lipton, 1988; Tauck, Frosch & Lipton, 1988; Karschin & Lipton, 1989).

Because recent evidence has indicated that vigorous treatment with enzymes, such as papain and trypsin, can possibly alter functional NMDA receptors (Vignon *et al.* 1982), the enzymatic dissociation procedure with papain solution was limited to 20 min. Under these conditions, the RGCs displayed substantial NMDA-activated currents (100–400 pA in whole-cell recordings in response to 200 μM NMDA at a holding potential of −60 mV).

Composition of solutions

Standard Hanks' balanced salt solution (HBSS) contained (mM): NaCl, 137; $NaHCO_3$, 1; Na_2HPO_4, 0·34; KCl, 5·36; KH_2PO_4, 0·44; $CaCl_2$, 1·25, $MgSO_4$, 0·5; $MgCl_2$, 0·5; Hepes, 5; glucose, 22·2; Phenol Red, 0·001% (v/v); pH adjusted to 7·2 with 0·3 N NaOH. Because Mg^{2+} produces ion-channel block of NMDA-activated currents (Nowak *et al.* 1984), Mg^{2+} salts were omitted from the standard HBSS, designated 'Mg^{2+}-free HBSS' throughout the experiments. The [Ca^{2+}] was adjusted to 2·5 or 0·1 mM with $CaCl_2$, termed 'Mg^{2+}-free, 2·5 Ca^{2+} HBSS' and 'Mg^{2+}-free, 0·1 Ca^{2+} HBSS', respectively. High (2·5 mM) Ca^{2+} was used when stable seals were needed for prolonged recordings, and 0·1 mM Ca^{2+} was used to reduce Ca^{2+}-dependent desensitization of NMDA-operated receptors when necessary (Mayer, Vyklicky & Clements, 1989). Glycine, excitatory amino acids, and various drugs were added to the Mg^{2+}-free solutions. Tetrodotoxin (TTX; 1 μM) was added to the extracellular solutions to block Na^+ channels. The standard CsCl intracellular solution for filling electrodes contained (mM): CsCl, 120; TEACl, 20; Hepes, 10; EGTA, 2·25; $CaCl_2$, 1; $MgCl_2$, 2; adjusted to pH 7·2 with 0·3 N NaOH (final [Na^+], 5 mM), and occasionally with 3 mM MgATP to minimize run-down in prolonged recordings (MacDonald, Mody & Salter, 1989). While TEA and Mg^{2+} can permeate and/or block NMDA-activated channels (Wright, Kline & Nowak, 1991), the concentration of each was kept constant in the presence or absence of memantine so this would not influence our conclusions about memantine's effects. For some experiments, Cs^+ in the intracellular solution was replaced by *N*-methyl-D-glucamine (NMDG), adjusted to pH 7·2 with HCl ([Cl^-], 125 mM); this was termed 'NMDG internal solution.' Osmolarity of all solutions was 300 ± 10 mosmol kg^{-1}.

Electrophysiological recordings

Experiments were performed at 28–31 °C, 4–8 h after retinal cultures were plated. Under these conditions, the vast majority of RGCs were ovoid and spatially compact, lacking neurites. The diameter of RGCs chosen for this study was between 12 and 18 μm. With this compact shape, firm attachment and ideal size, the RGC preparation is quite amenable to electrophysiological recording and fast solution changes, as described below. Whole-cell recordings were performed according to standard methods (Hamill, Marty, Neher, Sakmann & Sigworth, 1981). Patch pipettes were coated with Sylgard, fire polished and usually had a resistance of 1–4 MΩ in the bathing fluid when filled with CsCl intracellular solutions (Aizenman *et al.* 1988). The series resistance was below 10 MΩ and, if necessary, was compensated with the circuit of an EPC-7 patch-clamp amplifier (List Electronic, Darmstadt, Germany).

The majority of the experiments were performed with the whole-cell recording technique because of the complexity of single-channel behaviour of NMDA-gated channels, especially with relation to memantine (Chen *et al.* 1992). The liquid junction potential produced by NMDG internal solution was less than 2 mV and because of its small magnitude was not corrected for in the figures.

Solution changes and superfusion techniques

The recording dish was constantly superfused at a rate of 0·5–0·8 ml min^{-1} and contained a total volume of 100 μl. Fast solution changes were made via an array of 3–4 glass micropipettes (aperture diameter, 12–20 μm), placed 20–40 μm from the neuron under study and 200 μm apart from each other. For constant fluid ejection, pressure (3–9 p.s.i.) was applied to the pipettes by computer control. Rapid solution changes approximating a 'concentration jump' were then achieved by mechanically shifting the pipettes with a micromanipulator. While recording from solitary RGCs, the solution exchange time constant was 49·9 ± 1·9 ms ($n = 41$, means ± S.E.M.), as measured using [Na^+] jumps in the presence of kainic acid (Fig. 1*A*). The junction potential change measured with a cell-free patch electrode was faster, with a time constant of less than 2 ms (Fig. 1*B*). The slower solution change recorded in whole-cell experiments probably reflects superfusion of a much larger area of the cell surface compared with the faster exchange near the tiny opening of a patch pipette (Vyklicky, Benveniste & Mayer, 1990).

Data acquisition and analysis

Currents were recorded with an EPC-7 patch-clamp amplifier, digitized with a 12-bit, 125 kHz analog-to-digital converter (Data Translation), and viewed both on an analog oscilloscope (Tektronix) and a digital display module (Hewlett Packard). The sampling rate was 200–1000 Hz for whole-cell recording, and currents were filtered prior to digitization at 2–5 kHz (low pass) with an external filter (Ithaco, Bessel, 48 dB/octave). Voltage commands and data acquisition were controlled on-line by a PDP-11/73 computer (Digital Equipment Corporation). Data were displayed on a chart recorder (Gould) and stored on a 40 megabyte Winchester disk for later analysis.

The macroscopic blocking time constant (τ_{on}) and macroscopic unblocking time constant (τ_{off}) were measured by three methods:

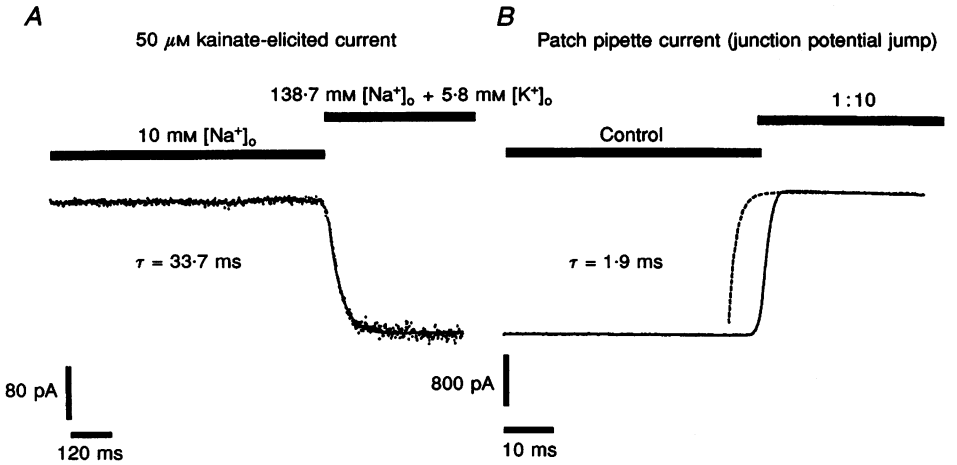

Figure 1. Fast solution exchange recorded using Na^+ concentration jumps and junction potential jumps

A, whole-cell recording of the response of a retinal ganglion cell (RGC) activated by 50 μM kainate and voltage clamped at −60 mV. The concentration jump was achieved by switching an extracellular solution of 10 mM Na^+ to a solution of 138·7 mM Na^+ plus 5·8 mM K^+. The relaxation, due to the increased chemical driving force for inward Na^+ current flowing through the kainate-gated channels, was fitted with a single exponential of time constant (τ), 33·7 ms. NMDG was used as a Na^+ substitute. *B*, change in current recorded using an open patch pipette that was voltage clamped at 0 mV during a switch to puffer solution diluted by 1:10 (in water) from normal Mg^{2+}-free 2·5 Ca^{2+} HBSS (Control). The relaxation, due to the change in junction potential, was fitted with a single exponential of τ, 1·9 ms (displaced dotted curve).

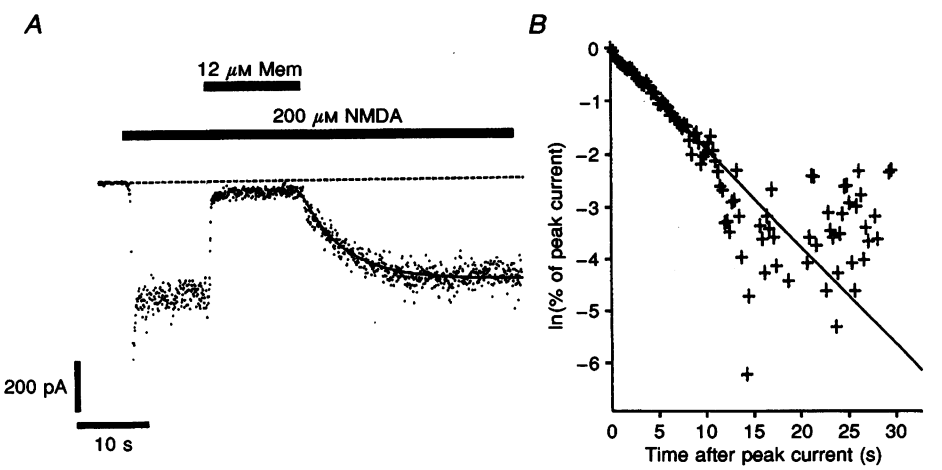

Figure 2. Representative exponential fit to the recovery phase from memantine inhibition of an NMDA-induced response

A, single exponential fit to the relaxation of the recovery phase from 12 μM memantine (here and in subsequent figures abbreviated to Mem) blockade during application of 200 μM NMDA (equation given in Methods section). For this current trace, the single exponential fit results in an unblocking time constant (τ_{off}) of 4·85 s. The time between the start of the recovery and 1/e of the amplitude of the decay is 4·95 s by direct measurement. The values of these time constants are very similar. *B*, the relaxation component of the current was sampled with 45 points, and the value of each point was then transformed to a logarithmic scale and plotted *vs.* time. The first 20 points of these transformed data were then fitted by linear regression, with a resultant time constant of 5·4 s. The scattered data points beyond 15 s would have heavily affected the accuracy of the regression fit, resulting in a misleading regression line. Therefore, the methods in *A* were used for the kinetic experiments in this work.

(i) The relaxation of memantine blocking and unblocking processes was fitted with a single exponential function:

$$I(t) = I(\infty) + [I(0) - I(\infty)] \exp(-t/\tau),$$

where $I(t)$ is the amplitude of the current at time t; $I(\infty)$, the current at steady state; $I(0)$, the amplitude of the current at time zero; τ, the time constant of decay, and $[I(0) - I(\infty)]$ is the amplitude of the time-dependent component of the response at the start of the relaxation. Both τ_{on} and τ_{off} were obtained from the fitted curves (Fig. 2*A*). (ii) The time between the start and 1/e of the decay of relaxation was measured directly and should equal the τ obtained from method (i), assuming that the relaxation indeed follows a single exponential process. (iii) The relaxation component of the current was sampled by a fixed number of points and transformed into a semilogarithmic plot *vs.* time (Fig. 2*B*). The transformed data were a linear function of time and could be fitted by linear regression reasonably well, indicating that the relaxation of memantine action approximated a single exponential process. However, the noise was always greater at steady-state current than during current decay, yielding higher variance for steady-state responses. The high variation for steady-state current produces undue weighting in linear regression fits, resulting in over-estimation of time constants. Hence, the values obtained from methods (i) and (ii) were always the same, while the value from method (iii) was always greater. However, the trend of voltage dependence of τ_{on} and τ_{off} was the same for all three methods. For clarity and convenience, the single exponential fit by method (i) is illustrated in all of the figures .

The data were fitted by a non-linear, least-squares method with weighting equal to the reciprocal of the variance of the data, using the iterative process of a Marquardt–Levenberg algorithm. During this fitting method, the dependence between parameters was constantly evaluated to ensure the validity of the equations, and the best fit for each set of data was then obtained and plotted for each graph.

RESULTS

Stoichiometry of memantine block

Dose–response analysis. At a holding potential of −60 mV, whole-cell currents of rat RGCs evoked by 200 μM NMDA were recorded before and during co-application of various concentrations of memantine. The percentage of residual current (normalized conductance or fractional response) was calculated by comparing the steady-state current during the co-application of memantine and NMDA (I_{Mem}) to the NMDA-evoked current before memantine application (I_{Con}). The percentage of residual current for various concentrations of memantine was then used to construct a dose–response curve for memantine blockade of 200 μM NMDA-elicited responses. The data were fitted by a non-linear least squares method with an empirical Hill equation as follows:

$$Y = 100 - \{Y_{max}/(1 + (IC_{50}/[Mem])^n)\}, \quad (1)$$

where Y is I_{Mem}/I_{Con} (%), Y_{max} is the maximum of this value, n is the empirical Hill coefficient, IC_{50} is the apparent 50% inhibition constant and [Mem] represents the concentration of memantine. This dose–response analysis resulted in an IC_{50} of 1·2 ± 0·2 μM (mean ± S.D., Fig. 3), a Y_{max} of 97 ± 5, and a Hill coefficient of 0·97 ± 0·12 (mean ± S.D.), suggesting one binding site for memantine action. The IC_{50} measured in this set of experiments was similar to the equilibrium dissociation constant (K_i) of 0·536 ± 0·035 μM (mean ± S.E.M.) reported by Kornhuber, Bormann, Retz, Hübers & Riederer (1989) for inhibition of [^{3}H]MK-801 binding in post-mortem human frontal cortex. Since these two values are very close, the IC_{50} of memantine antagonism will be presented as an apparent K_i of

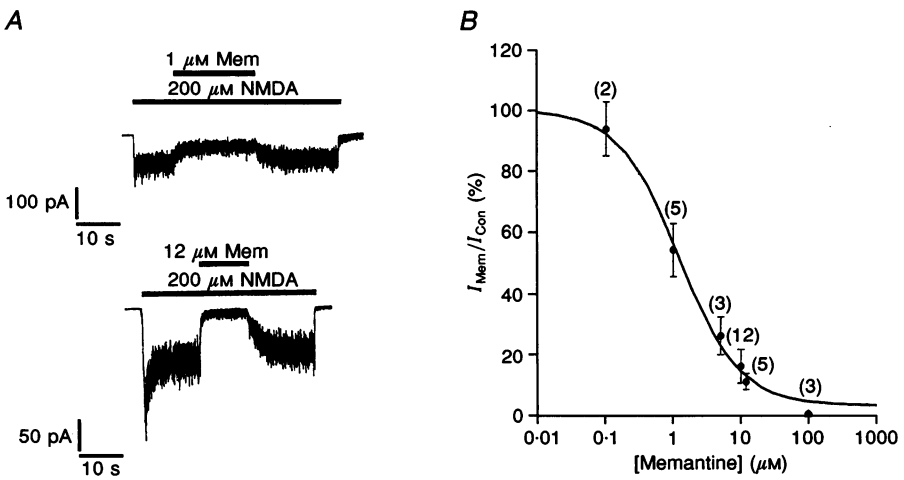

Figure 3. Dose–response analysis of memantine blockade of NMDA-evoked responses

A, blockade of 200 μM NMDA-activated currents by 1 and 12 μM memantine recorded from 2 different RGCs at a holding potential of −60 mV. The normalized conductance (I_{Mem}/I_{Con}) was used to construct a dose–response curve as in *B*. *B*, I_{Mem}/I_{Con} (%) *vs.* concentration of memantine. The data were fitted with eqn (1) by a non-linear least-squares method weighted by the reciprocal of the variance of each data point. Each data point was calculated from the number of cells in parentheses and is presented as the mean ± S.D.

memantine. Therefore, memantine appears to block NMDA-mediated responses with a potency less than that of phencyclidine but higher than that of ketamine (Sernagor, Kuhn, Vyklicky & Mayer, 1989; Wong & Kemp, 1991).

Bimolecular reaction of memantine blockade. The best fit of the memantine dose–response curve yielded an empirical Hill coefficient of approximately 1 (Fig. 3), which suggests a single binding site for memantine on each NMDA-gated channel. This result predicts a simple bimolecular reaction according to Scheme 1 (Anderson, MacKinnon, Smith & Miller, 1988):

$$\text{Channel} + \text{Mem} \rightleftharpoons \text{Channel-Mem (Blocked channel)}$$

Scheme 1

This simple bimolecular scheme predicts that the macroscopic blocking and unblocking actions of memantine proceeds with exponential relaxation, the macroscopic pseudo-first order rate constant of blocking (k_{on}) depends linearly on memantine concentration (as well as a constant, A), and the macroscopic unblocking rate (k_{off}) is independent of memantine concentration ([Mem]).

$$k_{on} = A[\text{Mem}], \quad (2)$$

$$k_{off}: [\text{Mem}] \text{ independent.} \quad (3)$$

These predictions were borne out experimentally (Fig. 4). Both macroscopic blocking and unblocking processes could be well fitted by a single exponential function (Fig. 4*A*). The macroscopic on-rate constant is the reciprocal of the measured time constant for onset (τ_{on}) and is the sum of the pseudo-first order blocking rate constant (k_{on}) and unblocking constant (k_{off}). The unblocking rate constant (k_{off}) is the reciprocal of the measured macroscopic unblocking time constant (τ_{off}). These transformations lead to eqns (4) and (5):

$$k_{on} = 1/\tau_{on} - 1/\tau_{off}; \quad (4)$$

$$k_{off} = 1/\tau_{off}. \quad (5)$$

The k_{on} calculated from eqn (4) increased linearly with memantine concentration with a slope factor of $(0{\cdot}4 \pm 0{\cdot}03) \times 10^6$ M^{-1} s^{-1} (mean ± S.D.), while the k_{off} from eqn (5) remained relatively constant with a Y-axis intercept of $0{\cdot}44 \pm 0{\cdot}1$ s^{-1} (Fig. 4*B*). A rapid method for validating this result can be obtained by estimating the equilibrium dissociation constant (K_i) for memantine action from the following equation:

$$K_i = k_{off}/(k_{on}/[\text{Mem}])$$

$$= Y\text{-axis intercept for } k_{off}/\text{slope factor for } k_{on}. \quad (6)$$

Equation (6) yields a K_i of 1·1 μM, which closely matches the K_i measured in the dose–response analysis and confirms the accuracy of this kinetic analysis. This result is consistent with the bimolecular process of Scheme 1 for the blocking action of memantine and indicates that a single molecule of memantine binds to an NMDA-gated channel. However, the slope factor for k_{on} and the Y-axis intercept are also affected by the open probability of the channel and will be further investigated in later sections.

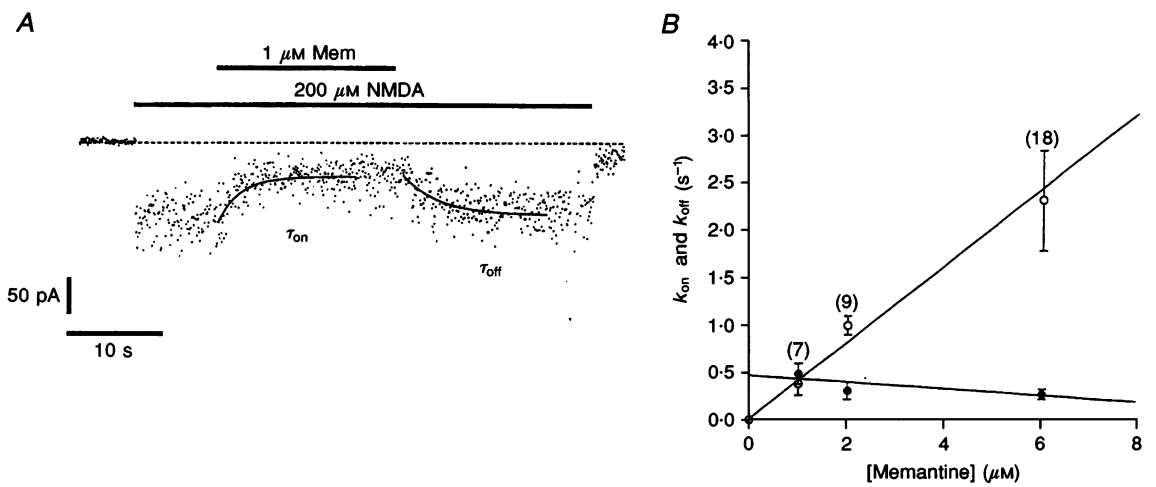

Figure 4. Bimolecular kinetics of memantine interaction

A, macroscopic relaxation for blocking and unblocking actions of memantine were well fitted by single exponentials to obtain the on-time constant (τ_{on}) and unblocking time constant (τ_{off}) for memantine inhibition . Values of k_{on} and k_{off} could then be calculated from eqns (4) and (5). Holding potential, −60 mV. *B*, kinetics of onset of and recovery from antagonism of 1, 2 and 6 μM memantine at a holding potential of −60 mV; k_{on} (○) and k_{off} (●) are plotted as a function of memantine concentration. Each point represents the mean ± S.D. for the number of cells shown in parentheses. The point at the co-ordinate (0,0) is constrained by definition since there is no k_{on} if no drug is present.

Lack of interaction of memantine with the fully closed, unliganded channel

An uncompetitive antagonist binds only to liganded channels. Thus, possible interactions with the fully closed, unliganded channel were used to help determine if memantine acted by a predominantly uncompetitive mechanism. Previous evidence strongly suggested that memantine preferentially binds to the open conformation of NMDA-gated channels (Chen *et al.* 1992). However, single-channel analysis showed that the major effect of memantine is to decrease the opening frequency of NMDA-operated channels. The reason for the decrease in opening frequency could be either that memantine also binds to the closed state or that memantine creates a blocked state that slowly recovers. The possibility that memantine also binds to a closed state of the channel was pursued further here. As shown in Fig. 3*A*, the activation of responses evoked by 200 μM NMDA and subsequent recovery after washout were much faster than the rate of memantine inhibition: the on-time constant for the response was 84·6 ± 5·1 ms ($n = 18$, mean ± S.E.M.), the off-time constant for washout was 152·3 ± 12·5 ms ($n = 11$), and both time constants were limited by the speed of solution changes in our system. These time constants were much shorter than the apparent association time constant of 2 μM memantine when channels were activated by 200 μM NMDA (~1 s) and the apparent dissociation time constant from activated channels (~3–4 s). This observation suggests a scheme in which the gating process of NMDA receptor-operated channels does not significantly contaminate measurements of the blocking and unblocking rates of memantine. Combined with the bimolecular nature of memantine blockade, a simple reaction mechanism that assumes that memantine interacts with both the closed and open states is presented as Scheme 2:

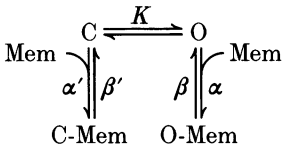

Scheme 2

In this Scheme, memantine is assumed to interact with the closed and open states with true second-order rate constants of association, α' and α, respectively. C represents the fully closed channel; O, the fully open channel initiated by NMDA binding; C-Mem, the closed/memantine-bound state; and O-Mem, the open but non-conducting state of the channel blocked by memantine. β and β' represent the off-rate constants for memantine from the open and closed states, respectively. K represents the equilibrium constant between states C and O. Since the gating kinetics of channel activation and deactivation are fast, a simple open probability (P_o) of the unblocked but closed channel can be assigned to indicate the weighted transformation from the closed to open state (Anderson *et al.* 1988). Quantitatively, the macroscopic pseudo-first order association rate constant of memantine (k_{on}) with the channel is the weighted sum (by P_o) of α and α' as in eqn (7):

$$k_{on} = \{\alpha' + P_o(\alpha - \alpha')\}[\text{Mem}], \quad (7)$$

$$\alpha' \gg 0 \rightarrow k_{on} = \{\alpha' + P_o(\alpha - \alpha')\}[\text{Mem}],$$

$$\alpha' \approx 0 \rightarrow k_{on} = P_o\alpha[\text{Mem}].$$

k_{on} simply depends on P_o and α when the association rate with the closed channel approaches zero. By varying the open probability over a wide range, binding to the closed state can be evaluated when P_o approaches zero.

A direct calculation of absolute P_o from single-channel recordings was obfuscated by the multiple conductance states of NMDA-gated channels (Howe, Cull-Candy & Colquhoun, 1991; Stern, Béhé, Schoeper & Colquhoun, 1992; Chen *et al.* 1992). The relative P_o was therefore computed from the response induced by various concentrations of NMDA. The current activated by NMDA usually follows the general equation of Ohm's law:

$$I = nP_{o,[\text{NMDA}]}g(V_h - V_{rev}), \quad (8)$$

where I is the whole-cell current; n, the total number of activatable channels on one cell; $P_{o,[\text{NMDA}]}$, the open probability at each concentration of NMDA; g, the single-channel conductance; V_h, the holding potential; and V_{rev}, the reversal potential for NMDA-gated channels, which is close to 0 mV under our recording conditions with CsCl internal solution. In any given cell, the ratio of current amplitude activated by various concentrations of NMDA to the current induced by 200 μM NMDA is equal to the ratio of $P_{o,[\text{NMDA}]}$ to $P_{o,200}$ and is designated as the relative P_o. This relative P_o can be obtained from the data of the dose–response analysis for NMDA-activated current in Fig. 5*A* and used for analysis in Fig. 5*C*. Additionally, the rate of blockade by 2 μM memantine was slower at 10 μM NMDA than at 200 μM NMDA (Fig. 5*B*). The k_{on} for memantine was calculated from eqn (4) (as in Fig. 4), and plotted against the relative P_o in Fig. 5*C*. This result clearly shows that k_{on} increases linearly with open probability and that k_{on} approaches a near-zero value when P_o approaches zero. Thus, the value of k_{on} for the closed channel state is very small (0·039; Y-intercept in Fig. 5*C*). This value is 25-fold slower than the k_{on} in the presence of 200 μM NMDA (~1 s^{-1} for 2 μM memantine). This extremely slow binding rate to the apparently closed state might reflect at least two possibilities: (i) memantine might reach the binding site in the channel pore through a hydrophobic pathway in the membrane, and (ii) residual, trace amounts of glutamate (remaining after wash with an HBSS micropipette) or the 2 μM glycine constitutively present in the bath solution might activate a low level of channel activity. The hydrophobic pathway of memantine seems very unlikely because intracellular memantine, at a saturating concentration of 100 μM, had no effect on NMDA-induced current nor on the

blocking effect of externally applied memantine over a range of holding potentials (Chen, 1992). However, residual glutamate surrounding solitary RGCs is probably negligible with the 'concentration-jump' technique that we used (see Methods). A low level of channel activity induced by the glycine in the bath solution may be the most plausible explanation because glycine alone was recently shown to activate recombinant heteromeric NMDA channels (Meguro *et al.* 1992; Monyer *et al.* 1992). Additionally, in our previous experiments (Fig. 1*B* in Chen *et al.* 1992), exposure to 12 μM memantine for 30 s in the absence of NMDA and glycine did not inhibit the response induced by the subsequent application of 200 μM NMDA. Since the apparent association time constant of 12 μM memantine is 200 ms (Fig. 1*A* in Chen *et al.* 1992), the observed k_{on} of memantine for the closed channel is at least 100-fold slower than the k_{on} of memantine for the channel in the presence of 200 μM NMDA. Taken together, these data argue that memantine at low micromolar concentrations does not significantly interact with the closed, unliganded state of the channel and acts as a 'pure' uncompetitive antagonist.

Trapping memantine in the closed channel

In order to quantify the influence of open probability (P_o) and internal permeant cations on the voltage dependence of memantine action, a more precise scheme for the drug's mechanism of antagonism was sought. We found that recovery from memantine blockade required the re-application of NMDA, indicating that the channel can close and trap memantine in a blocked but unliganded state (Fig. 6*A*). In order to extend Scheme 2 to include the trapping protocol but avoid contamination of the measurement of k_{off}, the gating process of the blocked channel has to be faster than the kinetics of memantine action. We used a low concentration of memantine (2 μM) to slow k_{on} in order to demonstrate clearly the difference in the gating process and the kinetics of memantine inhibition. The response to 200 μM NMDA was first blocked by co-application of memantine and NMDA, and then the RGC was exposed immediately to a solution lacking agonist or memantine. Following this protocol, a fast off-phase with a time constant of 152 ± 24 ms was observed upon washout of agonist plus memantine (Fig. 6*A*, left). This value is not

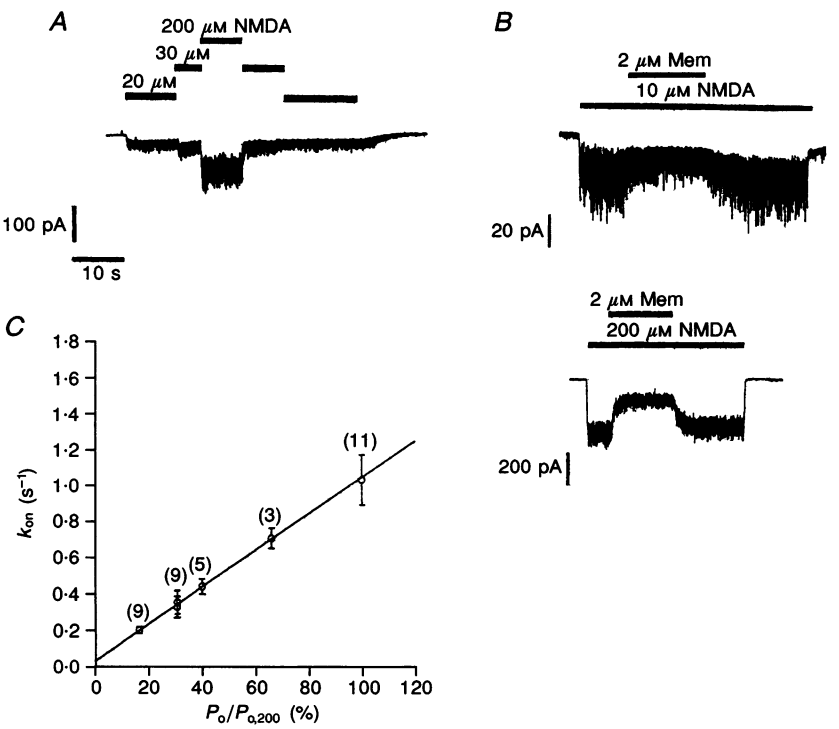

Figure 5. Macroscopic pseudo-first order blocking rate constant of memantine *vs.* relative open probability of NMDA-gated channels

A, dose–response data of NMDA-induced responses from RGCs. Whole-cell currents activated by NMDA in one RGC at −60 mV are shown as an example. The currents induced by various concentrations of NMDA were normalized to the current amplitude evoked by 200 μM NMDA (I/I_{200}%) in order to obtain the relative open probability ($P_o/P_{o,200}$) to be plotted in *C*, below. *B*, two representative current traces induced by 10 and 200 μM NMDA at −60 mV illustrate that the onset of inhibition by 2 μM memantine is faster for higher concentrations of NMDA. *C*, macroscopic pseudo-first order blocking rate (k_{on}) increases linearly with relative open probability ($P_o/P_{o,200}$). The relative open probability was calculated from the dose–response data for NMDA-evoked currents in *A*. Each point represents the mean ± S.D. of the values for the number of cells indicated in parentheses. The linear fit of the data resulted in a slope factor of 0·01 ± 0·00016 s^{-1} and *Y*-intercept of 0·039 ± 0·005 s^{-1} (mean ± S.D.).

statistically different from the off-time constant for washout of NMDA alone. After a washout period of 11·3 s, subsequent application of NMDA alone induced fast activation of a smaller inward current than observed previously with a time constant of 80 ± 12 ms, which is not statistically different from the on-time constant for activation of unblocked channels. Thus, this fast activation component represents the opening of unblocked channels, and it was followed by a slow relaxation to the previously observed level of NMDA-evoked current with a time constant similar to the τ_{off} of slow recovery from memantine blockade (Fig. 6*A*, right). Since the slow relaxation began at a current level equivalent to that seen when 2 μM memantine was applied to block the NMDA response, the channels must have remained blocked during the prior washout period. These results illustrate that (i) agonist can dissociate from the receptor and trap memantine in the blocked channel; (ii) memantine can only leave the binding site when the receptor is re-activated by NMDA; and (iii) agonist binds and dissociates from the blocked channel at a faster rate than that of memantine.

Taken together, these facts can be used to extend Scheme 2 to a new working scheme (Scheme 3 in Fig. 6*B*) with the following kinetic parameters: C and O represent the closed and open states of the channel, respectively; O-Mem, the blocked, liganded but non-conducting channel; C*-Mem, the blocked, unliganded and memantine-trapped channel; α, the microscopic on-rate constant; β, the microscopic off-rate constant; [Mem], the concentration of memantine; K and K', the equilibrium constants for opening of the unblocked channel (C) and blocked but closed channel (C*-Mem), respectively. In Scheme 3, we assume that the gating process of both blocked and unblocked channels is faster than the kinetics of antagonist action, an assumption that was empirically borne out (see below). Thus, the macroscopic unblocking rate constant (k_{off}) of memantine can be defined as follows:

$$k_{off} = 1/\tau_{off} = \beta P_o'. \quad (9)$$

The pseudo-first order blocking rate constant (k_{on}) of memantine would be as follows:

$$k_{on} = 1/\tau_{on} - 1/\tau_{off} = \alpha P_o[\text{Mem}], \quad (10)$$

where P_o and P_o' are the open probability of the unblocked channel and the blocked but closed channel, respectively. Using eqns (9) and (10), a more sophisticated kinetic analysis can be undertaken.

Using this analysis, we show below that memantine binding stabilizes the open conformation of the blocked channel and does not affect the affinity of the ligand. The transformation

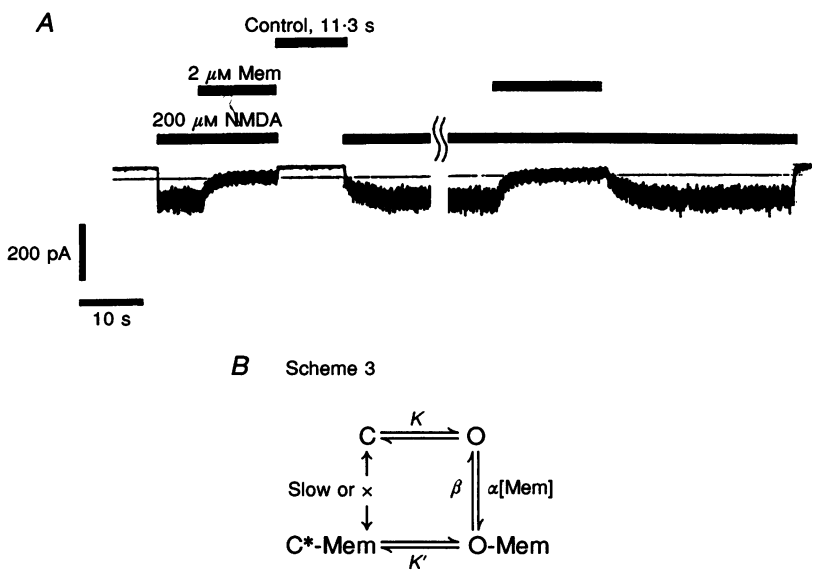

Figure 6. A trapping scheme for memantine inhibition

A, the response to 200 μM NMDA was first blocked by 2 μM memantine at −60 mV, and then both agonists and antagonists were washed out by exposing the cell suddenly to a solution containing only the control solution for 11·3 s to demonstrate the trapping phenomenon and the fast closing phase of the blocked channel (left). After washout by the control solution, a second application of NMDA alone displayed a fast-rising phase of channel activation followed by a slow relaxation from the recovery of memantine blockade. The slow relaxation was similar to the regular recovery phase from memantine block without the trapping protocol, as shown on the right. The control solution was Mg^{2+}-free, 0·1 Ca^{2+} HBSS with 2 μM glycine. The blocking time constant for memantine (τ_{on}) was 1·1 s for this cell. *B*, proposed trapping scheme for memantine antagonism. See text for details. × indicates that leak of memantine out of the blocked, closed and memantine-trapped channel is essentially negligible.

between C*-Mem and O-Mem in Scheme 3 is a 'hidden' process and is not readily observable. However, the open probability of the blocked channel (P_o') is a component of the macroscopic unblocking rate constant (k_{off}), and k_{off} therefore can be used to study the possible effect of memantine binding on P_o'. In Fig. 7 the unblocking rate constant, k_{off}, could be reliably measured at a holding potential of −60 mV in the presence of $\geqslant 10$ μM NMDA (as in Fig. 5). At concentrations of NMDA below 10 μM, both the degree of blockade by memantine and the amplitude of the NMDA-activated currents were too small for accurate kinetic analysis. An alternative method to estimate P_o' was therefore used for NMDA concentrations < 10 μM, based upon the analysis of Ba^{2+} blockade of Ca^{2+}-activated K^+ channels by Miller *et al.* (1987): the channel opens infrequently in the presence of very low concentrations of NMDA, which allows some recovery of channels previously blocked by memantine. The probability of remaining blocked, P_b, in the presence of low levels of receptor activation by NMDA can be described by eqn (11):

$$P_b = \exp(-k_{off}\Delta t), \tag{11}$$

where Δt is the duration of exposure to low concentrations of NMDA after memantine blockade. Since k_{off} is equal to $\beta P_o'$, then P_o' at low [NMDA] can be expressed as a function of measurable quantities:

$$\beta P_o' = -(\ln P_b)/\Delta t. \tag{12}$$

In a typical experiment (Fig. 7*A*), the responses to 200 μM NMDA were first blocked by 12 μM memantine, and the amplitude of the blocked current (I_a) was measured. After steady-state blockade had been achieved, the cell was suddenly exposed to a solution with 1 μM NMDA alone for the duration, Δt, following which 200 μM NMDA alone was re-applied to the cell. The recovery phase observed upon re-application of 200 μM NMDA could be fitted with a

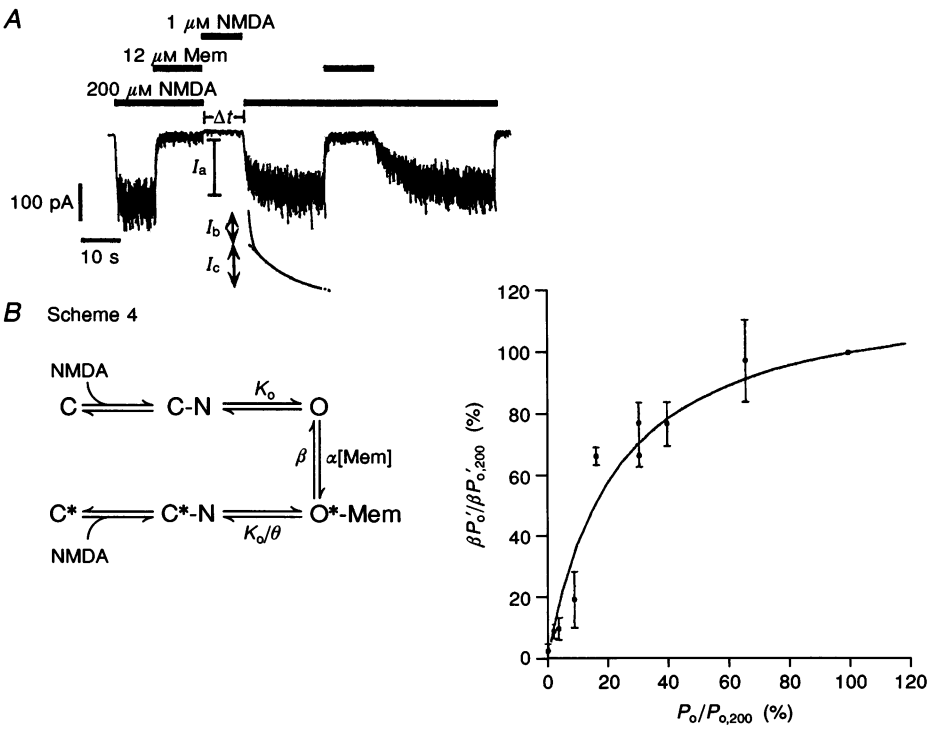

Figure 7. Memantine binding stabilizes the open conformation of the blocked channel

A, the response to 200 μM NMDA was first blocked by 12 μM memantine (left; I_a is the blocked portion of the current) and then exposed rapidly to a solution with a low concentration of NMDA (1 μM in this figure) to permit partial recovery during a time period, Δt. The partial recovery was then evaluated by the relative proportion of slow (I_c) and fast relaxation (I_b) upon the re-application of 200 μM NMDA alone (right). The slow relaxation represents the portion of current remaining blocked during Δt and was used to calculate $\beta P_o'$. *B*, uncompetitive scheme of memantine action and high open probability for the blocked channel (P_o'). $K_o = [O]/([C] + [C\text{-}N])$ and $P_o = [O]/([C] + [C\text{-}N] + [O])$. The data measured by the methods illustrated in *A* are shown at the right and fitted by non-linear least squares with the equation, $Y = (a_m + 100)\{X/(a_m + X)\}$. The fit yields an a_m of 22·97. θ was then calculated from k_{off} and k_{on}, which were measured with 200 μM NMDA and 1 μM memantine, and resulted in a value of 0·146. Note that at $P_o/P_{o,200} = 30\%$ (corresponding to 10 μM NMDA), two data points are shown that were calculated by the two methods described in the text; the two values agree relatively well.

double exponential function (the displaced curve in Fig. 7*A*). This analysis revealed a fast component (I_b), representing the activation of channels which had been unblocked during time Δt, and a slow component (I_c), representing the recovery of channels that had remained in the blocked state. Additionally, as Δt is varied, P_b ($= I_c/I_a$) behaves as a single exponential function of Δt. By measuring the proportion of channels that had remained blocked, $\beta P_o'$ at very low concentrations of NMDA is obtained (eqn (12)) and can be normalized to $\beta P_{o,200}'(k_{off,200})$, measured with 200 μM NMDA. This calculation results in the normalized open probability of the blocked channel ($P_o'/P_{o,200}$). However, the absolute value of P_o' is still not directly available.

By assuming that the affinity of NMDA for its receptor is not changed by the occupation of its associated channel by memantine and that the equilibrium constant (K_o) for opening in the unblocked state differs from that of the blocked state by a constant factor, $1/\theta$, analogous to the 'stabilization factor' of Miller *et al.* (1987), Scheme 3 can be further developed as Scheme 4 (Fig. 7*B*). Here, C is the closed and unliganded channel; C-N, the liganded but closed channel; O, the open state of the channel; O*-Mem, the open but blocked channel; C*-N, the closed, liganded and blocked channel; C*, the unliganded, closed and blocked channel; and α, β and [Mem] have the same definitions as in Scheme 3. With Scheme 4 and the assumptions implicit in K_o, P_o' can be expressed as a function of P_o (after Miller *et al.* 1987):

$$P_o' = P_o/[\theta + (1 - \theta)P_o] \quad (13)$$

and

$$P_{o,200}' = P_{o,200}/[\theta + (1 - \theta)P_{o,200}].$$

By applying eqn (13) to the equilibrium state of Scheme 4, the normalized P_o' (represented by the percentage, $P_o'/P_{o,200}'$) can then be expressed as a function of the normalized P_o (note, eqn (15) is derived by replacing P_o' and $P_{o,200}'$ in eqn (14) with eqn (13)):

$$Y = P_o'/P_{o,200}', \; X = P_o/P_{o,200}, \quad (14)$$

$$Y = (a_m + 100)\{X/(a_m + X)\},$$

$$\text{and } a_m = 100\theta/[(1 - \theta)P_{o,200}], \quad (15)$$

where Y and X are percentages and a_m is a mathematical construct with no physical meaning. The measured and normalized values of the open probability of the blocked

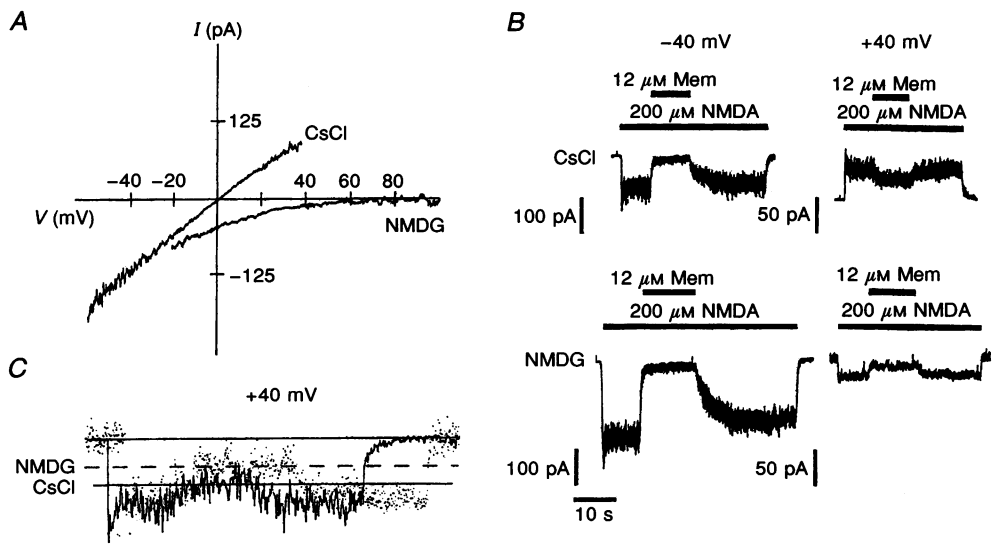

Figure 8. Effect of removal of internal permeant caesium (Cs^+) on memantine antagonism

A, *I–V* curves were produced by 614·4 ms voltage ramps from −60 to +40 mV for CsCl internal solution and by 1·024 s voltage ramps from −20 to +100 mV for the NMDG internal solution. *I–V* curves obtained in the absence of agonists were subtracted from those acquired during the steady-state component of the agonist-activated currents. Digitized data points were the mean of 8 consecutive ramp recordings. The *I–V* curve recorded with CsCl internal solution was fitted by linear regression and resulted in a reversal potential of 2·6 mV, which is close to the theoretical V_{rev} of 3·8 mV calculated from the Nernst equation assuming equal permeability of Na^+, K^+ and Cs^+. The *I–V* curve recorded with the NMDG internal solution intercepted the voltage axis at +70 to +80 mV. *B*, responses induced by 200 μM NMDA and antagonized by 12 μM memantine at −40 and +40 mV from 2 cells recorded in the presence of internal Cs^+ (top row) or its absence (bottom row). *C*, an NMDA response recorded with CsCl internal solution at +40 mV (continuous trace) was inverted and scaled down to superimpose at maximum amplitude on a response recorded with NMDG internal solution at +40 mV (dotted trace). A continuous line for the recording with CsCl and a dashed line for the recording without internal Cs^+ were drawn to indicate the levels of residual current during memantine blockade.

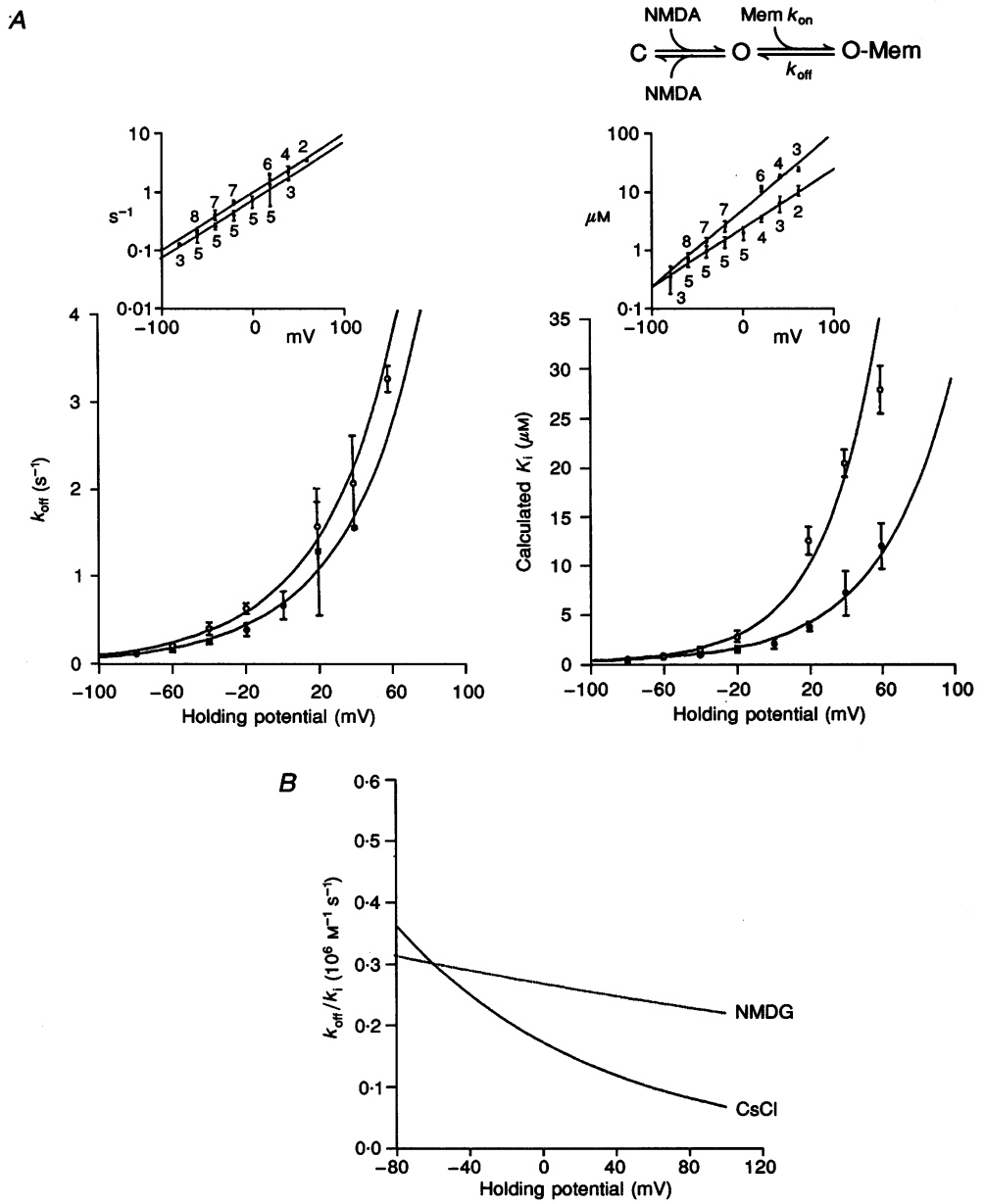

Figure 9. Effect of removal of internal permeant caesium ions on the k_{off} and K_i of memantine inhibition

A, voltage dependence of k_{off} (or $1/\tau_{off}$, left) and K_i (right) in the presence of internal Cs^+ (○) or its absence (●). The measurement and calculation of k_{off} were the same as Fig. 4, and K_i was calculated from the same scheme (top right) as in Fig. 2 of Chen *et al.* (1992) with the following equations:

$$K_i = k_{off}/k_{on} \text{ and } I_{Con}/I_{Mem} = 1 + ([Mem]/K_i)/(1 + K_d/[NMDA]).$$

A semilogarithmic transformation of each plot is shown as an inset (above) to demonstrate the voltage dependence. Each data point represents the mean ± S.D. for the number of cells indicated. The points were fitted by linear regression ($r^2 > 0{\cdot}99$). The marked change in the voltage dependence of K_i after the removal of internal Cs^+ is clearly illustrated in the semilogarithmic plot. *B*, plot of k_{off}/K_i to estimate the voltage dependence of the product of the microscopic on-rate constant (α) multiplied by the open probability of the unblocked channel (P_o). The function of αP_o in terms of voltage was obtained from eqn (17). The curves were generated by computer over the potential range of −80 to +100 mV for recordings with CsCl or NMDG internal solution. Values used for calculation were as follows: k_{off} (CsCl): $0{\cdot}894 \times 10^{0{\cdot}00973V}$; K_i (Cs^+): $5{\cdot}202 \times 10^{0{\cdot}01378V}$; k_{off} (NMDG): $0{\cdot}667 \times 10^{0{\cdot}009779V}$; K_i (NMDG): $2{\cdot}494 \times 10^{0{\cdot}010645V}$; αP_o (CsCl): $0{\cdot}172 \times 10^{-0{\cdot}00405V}$; αP_o (NMDG): $0{\cdot}267 \times 10^{-0{\cdot}000866V}$.

Table 1. Summary of voltage-dependent parameters of K_i, k_{off} and k_{on} for memantine action

	δ (calculated from K_i)	K_i e-fold change (mV)	k_{off} e-fold change (mV)	k_{on} e-fold change (mV)
CsCl	0·83 ± 0·07	32·0 ± 2·4	53·3 ± 4·1	43
NMDG	0·53 ± 0·04	49·7 ± 3·1	49·5 ± 2·6	—

The data for the voltage dependence of K_i and k_{off} are from a total of 8 sets of experiments with CsCl or NMDG internal solution using the same experimental protocol. Values are presented as means ± S.E.M. The voltage dependence of k_{on} was determined from a separate set of experiments, calculated as in Fig. 4. δ represents the fraction of the transmembrane voltage sensed by memantine, as calculated from the Woodhull equation (Woodhull, 1973).

channel ($P_o'/P_{o,200}'$) are plotted against the normalized open probability of the unblocked channel ($P_o/P_{o,200}$) in Fig. 7*B*. This graph shows that $P_o'/P_{o,200}'$ varies with $P_o/P_{o,200}$ along a rectangular hyperbola, as predicted from eqn (15). The non-linear least-squares fit to these data yields a value of a_m of 22·97. By combining eqns (9), (10), (13) and (15), the ratio of k_{off} to k_{on} at −60 mV for inhibition of responses induced by 200 μM NMDA by a fixed concentration of memantine can be shown to be a function of a_m and θ:

$$k_{off,200}/k_{on,200} = (\beta P_{o,200}')/(\alpha P_{o,200}[\text{Mem}]) = K_i/[\text{Mem}]\{a_m/[(a_m + 100)\theta]\}. \quad (16)$$

At a low concentration of memantine (1 μM), which allowed us to slow down the blocking rate and obtain efficient washout, k_{on} and k_{off} could be measured accurately (0·476 s^{-1} for $k_{off,200}$ and 0·371 s^{-1} for $k_{on,200}$ at −60 mV). These empirically derived kinetics of memantine antagonism were then used for calculating θ. Given memantine's K_i of ~1 μM and the value of a_m obtained above, we calculated θ from eqn (16) to be 0·146. This value of θ indicates that memantine binding inside the pore shifts the open–closed equilibrium toward channel opening by ~4·81 kJ mol^{-1} (Miller *et al.* 1987). In other words, an NMDA channel with a memantine molecule inside it is open more often than when it is unoccupied by the blocker.

This interpretation relies on the assumption that the gating process of blocked and unblocked channels is fundamentally similar, separated by only a fixed free energy. To test this assumption utilizing the derived value of θ and Scheme 4, we generated a computer-simulated prediction for the NMDA dose–response curve in the presence of memantine based upon the measured dose–response curve obtained in the absence of antagonist (from Fig. 5*A*). We then compared this predicted dose–response curve in the presence of antagonist to that obtained experimentally and found a very good fit with no change in the apparent affinity of NMDA (for details of the computer simulation and figures, see Chen, 1992). Thus, our assumptions appear to be valid, supporting the notion that the binding energy of memantine stabilizes the open (but blocked) channel conformation without affecting agonist affinity and thus without cooperativity of the ligand binding process. Taken together, these results suggest that memantine acts by pure uncompetitive antagonism. This mode of action may be advantageous for therapeutic intervention (see Chen *et al.* 1992).

Removal of internal Cs^+ does not affect the voltage dependence of k_{off} but increases the association rate of memantine

In a series of experiments, internal permeant caesium ions were replaced with equimolar NMDG. The permeability of NMDG through NMDA-gated channels was assessed by recording with a voltage-ramp protocol in Mg^{2+}-free, 0·1 Ca^{2+} HBSS extracellular solution (Fig. 8*A*). The *I–V* curve recorded with standard CsCl internal solution had a reversal potential (V_{rev}) of 2·6 mV, but with NMDG internal solution there was essentially no outward current until approximately +80 mV. Assuming NMDA receptor-operated channels are not permeated by NMDG, the theoretical V_{rev} calculated from the Nernst equation is +83 mV, which is very close to the experimental result. Therefore, these data strongly support the notion that NMDG does not significantly permeate NMDA-gated channels under these conditions and is a good substitute for Cs^+ to test the effect of internal permeant ions on the voltage dependence of the k_{off} for memantine (see also MacDonald *et al.* 1991).

Memantine (12 μM) effectively blocked the NMDA-induced current with NMDG internal solution even at +40 mV (Fig. 8*B*, bottom row), while only slight blockade was observed for recordings with CsCl internal solution (Fig. 8*B*, top row). In Fig. 8*C*, the current recorded at +40 mV with the CsCl internal solution (continuous trace) was scaled (×0·58) and reversed in polarity to superimpose on the current recorded with NMDG internal solution (dotted trace). These superimposed traces illustrate that memantine blocked NMDA-evoked responses to a greater degree without internal Cs^+ (dashed line) than with internal Cs^+ (continuous line). However, the macroscopic unblocking rate constant (k_{off}) manifests the same voltage dependence in the presence and absence of internal Cs^+ (Fig. 9*A*, left). From the results of four sets of similar experiments, k_{off} was found to undergo an e-fold change per 53·3 ± 4·1 mV

(mean ± S.E.M.) with CsCl internal solution and 49·5 ± 2·6 mV with NMDG internal solution (summarized in Table 1). The absolute value of k_{off} at each holding potential was slightly reduced by removal of internal Cs^+, but the difference was not statistically significant (by an analysis of variance and Scheffé's *post-hoc* multiple comparisons of means).

Surprisingly, the K_i for memantine became less voltage dependent when the internal Cs^+ was removed (Fig. 9*A*, right). From four sets of similar experiments in the presence of NMDG internal solution, the calculated K_i for memantine on 200 μM NMDA-induced current displayed an e-fold change per 49·7 ± 3·1 mV (mean ± S.E.M.), and the predicted memantine binding site sensed 53 ± 4% of the transmembrane potential field. In contrast, the K_i with CsCl internal solution exhibited an e-fold change per 32·0 ± 2·4 mV, and the predicted binding site sensed 83 ± 7% of the transmembrane potential (data summarized in Table 1). Since the K_i represents the ratio of the macroscopic off-rate constant ($k_{off} = \beta P_o'$) to the macroscopic on-rate constant ($k_{on} = \alpha P_o$), and the voltage dependence of k_{off} is not affected by the removal of the internal Cs^+ ions, then the change in voltage dependence of K_i produced by internal Cs^+ ions must reside in αP_o and can be estimated from the following equation:

$$\alpha(V)P_o = k_{off}(V)/K_i(V), \quad (17)$$

where α, k_{off} and K_i are expressed as a function of voltage. The equation for k_{off} and K_i as a function of voltage can be obtained by a regression fit to the data shown in Fig. 9*A*. By applying the transfer function in eqn (17), $\alpha(V)$ can be expressed in terms of voltage to demonstrate the change in voltage dependence of $\alpha(V)P_o$ after the removal of internal Cs^+ ions. Using this method, Fig. 9*B* illustrates that the voltage dependence of $\alpha(V)P_o$ dramatically decreased in the absence of internal Cs^+.

Since the voltage dependence of k_{off} ($= \beta P_o'$) does not change after removal of internal Cs^+ and since there is no evidence to suggest that NMDG affects the open probability of the channel in a voltage-dependent manner, the voltage dependence of P_o' and thus also P_o probably do not change following replacement of Cs^+. Thus, reduction in internal Cs^+ appears to predominantly decrease the voltage dependence of the on-rate constant (α) rather than the microscopic off-rate constant (β) for memantine action. Further, in the presence of internal Cs^+ the value of α became smaller with depolarization (Fig. 9*B*). This voltage-dependent decrease in α gradually dominates the permeation pathway as the membrane potential is depolarized and resembles the inhibition of memantine binding produced by increased binding of internal permeant ions. A similar effect on permeation has been shown for Ba^{2+} blockade of the Ca^{2+}-activated K^+ channel in which the increasing trans (external) K^+ concentration greatly reduced the blocking rate of internal Ba^{2+} but had no effect on its unblocking rate (Vergara & Latorre, 1983). Taken together with the aforementioned results, this effect of internal permeant ions on memantine action would be difficult to reconcile with models in which memantine binds to a site outside the Cs^+ permeation pathway.

If memantine indeed binds inside the channel pore, the on-rate constant (α) of the drug should also sense at least part of the transmembrane potential, but probably not as much as the unblocking rate constant because of the possible interaction of memantine with permeant ions in the conduction pathway. Nonetheless, Fig. 9*B* shows that the value of αP_o was almost voltage independent when internal Cs^+ was replaced with impermeant NMDG. One must take into account, however, the fact that the open probablity (P_o) increased with depolarization and could have negated a decrease in α with depolarization. Additionally, we know from previous work that the increase in nP_o is observed over a *slow* time course following depolarization from negative holding potentials (Nowak & Wright, 1992). Therefore, we rapidly (within 6 min) performed measurements of the blocking rate (k_{on}) of 6 μM memantine in each of seven cells at −60 to −20 mV. This method ensured the stability of nP_o, representing a probability-clamp technique, and minimized the influence of P_o on the voltage dependence of the on-rate of memantine. Using this rapid protocol of recording, k_{on} (or αP_o) was found to be voltage dependent and changed e-fold per 43 mV. This significant voltage dependence of k_{on} in the face of predominantly inward currents is very difficult to explain by an effect mediated by internal permeant cations. Therefore, the on-rate of memantine inhibition is probably voltage dependent. The voltage dependence of k_{off} and K_i after removal of internal Cs^+, taken together with the voltage dependence of k_{on} when P_o is relatively stable and all currents are inward, suggests that the memantine blocking site is most likely to be inside the channel pore.

DISCUSSION

The major lines of evidence usually mounted to support a mechanism of open-channel block by an NMDA antagonist include (i) voltage- and use-dependent inhibition, and (ii) a dramatic decrease in the opening frequency as well as a slight decrease in the mean channel open time, as observed in single-channel recordings (Sernagor *et al.* 1989; Chen *et al.* 1992). However, the modes of antagonism encompassed by the terms 'uncompetitive' and/or 'non-competitive' are not necessarily interchangeable with open-channel blockade. From the pharmacological point of view, it appears to be the uncompetitive mode of action, not the feature of 'open-channel blockade' *per se*, that confers a therapeutic benefit to a drug's antagonistic action: the action of an uncompetitive inhibitor is contingent upon prior activation of the receptor by the agonist, and therefore the degree of antagonism increases as the level of agonist increases. This characteristic leads to the potential clinical benefit of relatively sparing

normal neurotransmission while blocking excessive (pathological) activation of channels by escalating levels of agonist (Chen *et al.* 1992; reviewed in Lipton, 1993).

In this light, it is important to determine whether a drug such as memantine has a truly pure uncompetitive nature in addition to its previously known mechanism of open-channel block (Chen *et al.* 1992). A pure uncompetitive antagonist has to fulfill the following criteria: (i) antagonist binding does not change agonist affinity (no co-operativity), and (ii) antagonist binding to and exiting from the receptor occurs only in the presence of agonist. In the present study, we have attempted to establish a sequential method to elucidate the uncompetitive rather than non-competitive nature of antagonism by the open-channel blocker, memantine. We also sought to establish the molecular characteristics of the interaction of memantine with the NMDA-gated channel. We chose memantine for this study because it is known to be tolerated clinically by humans (for references, see Chen *et al.* 1992), and we sought to unravel the underpinnings of this therapeutic advantage in terms of molecular pharmacology. Our results lead to five major conclusions.

First, memantine blocks 200 μM NMDA-evoked responses with a K_i of $\sim$1 μM at -60 mV, and the antagonism follows a bimolecular reaction process (Fig. 4); one molecule of memantine binds to a site in the channel and causes inhibition. This 1:1 stoichiometry is supported by the fact that the macroscopic blocking rate of memantine increases linearly with concentration and the macroscopic unblocking rate is independent of memantine concentration. Both the blocking and unblocking rates of memantine action can be described by a single exponential process. In addition, externally applied memantine most probably interacts with the channel directly and does not go through the membrane to act on a cytoplasmic site of the NMDA-gated channel due to the lack of influence of 100 μM intracellular memantine.

Second, from a kinetic analysis memantine binds preferentially to the open, liganded conformation of the NMDA-gated channel and interacts very slowly, if at all, with the closed, unliganded state of the channel (Fig. 5). As the open channel probability (P_o) approaches zero, there is only a very small effect of memantine, possibly explained by residual amino acids in the superfusion medium. This analysis strongly supports the notion that memantine acts in an uncompetitive manner because its binding requires prior activation of the receptor.

Third, open-channel blockade of NMDA-activated current by memantine can be well described with a trapping scheme similar to the model proposed previously to explain blockade of Na^+ channels in squid axons by the channel blocker QX222 (Starmer, Yeh & Tanguy, 1986; Starmer, Packer & Grant, 1987). The agonist dependence of onset and recovery from memantine blockade indicates that the action of memantine is contingent upon prior activation of the channel by NMDA (Chen *et al.* 1992). Memantine can be trapped within the channel if it is suddenly closed by fast washout of the agonist (Fig. 6). This result is reminiscent of the blockade of the open state of Ca^{2+}-activated K^+ channels by Ba^{2+} (Miller, 1987; Miller *et al.* 1987). Furthermore, the trapping phenomenon supports the hypothesis that agonist binds and dissociates from the blocked channel at a faster rate than that of memantine. Taken together, these facts allow us to establish a trapping scheme of memantine action for further kinetic analysis.

Fourth, by developing Scheme 4 we show that memantine blockade stabilizes the open conformation of the channel by 4·81 kJ mol^{-1} over the open/unblocked channel and does not affect ligand binding affinity. For the Ca^{2+}-activated K^+ channel, Miller *et al.* (1987) demonstrated that the binding of Ba^{2+} at a blocking site inside the channel pore increases the open probability of the blocked channel over the unblocked channel and has no effect on the intrinsic channel gating process. For a ligand-gated channel, the situation is slightly more complicated: the occupancy of the ion pore by a blocker could affect either the opening–closing process of the channel or the ligand-dependent activation of the receptor, e.g. ligand binding affinity, and as a consequence lead to a change in the open probability of the blocked channel. We found that memantine stabilizes the open conformation of blocked NMDA channels to a lesser degree than Ba^{2+} on Ca^{2+}-activated K^+ channels, but in a similar fashion. This stabilization of the open conformation by memantine was further suggested by the agreement between the predicted and measured dose–response curves for NMDA in the presence of 2 μM memantine. This agreement lends credence to the hypothesis that the agonist-dependent activation process is similar whether or not the channel is blocked by memantine.

The kinetic information regarding the mode of action of memantine can be used to distinguish its uncompetitive nature from non-competitive antagonism. Based on simple schemes for pure non-competitive (Fig. 10*A*) and uncompetitive behaviour (Fig. 10*B*), a computer simulation for each type of antagonism is shown in Fig. 10*C*. In pure non-competitive antagonism, the blocker (here, memantine) binds to the open-liganded and closed-unliganded states of the channel with equal potency and does not affect the affinity of the agonist. In order to maintain microscopic equilibrium in a non-competitive scheme, the open probability of the blocked channel has to be the same as the open probability of the unblocked channel. This non-competitive action will result in the same degree of blockade irrespective of the concentration of agonist (dotted line, Fig. 10*C*). In contrast, pure uncompetitive antagonism predicts a change in the open probability of the blocked channel and gives rise to a greater degree of blockade with increasing concentrations of agonist (continuous line, Fig. 10*C*) (for references, see Chen *et al.* 1992). The major distinguishing feature between these two types of

antagonism is the different rates of interaction of the blocker with the open and closed states of the channel. In pure uncompetitive antagonism, the rate of interaction with the closed channel is zero. The good fit of the memantine data to the theoretical curve (Fig. 10*C*) strongly suggests that the mode of memantine action is principally uncompetitive.

Recent evidence indicates the association rate of open-channel blockers is mainly diffusion limited in a fixed ionic environment, while the dissociation rates from the blocking sites vary and largely determine the binding affinity. Wang (1990) showed that values of the apparent k_{on} of different local anaesthetics differ only by ~2-fold, while values of the apparent k_{off} differ by ~20-fold and therefore are the major determinant of the value of K_d. MacDonald *et al.* (1991) also showed that the apparent forward rate constants are similar for ketamine, phencyclidine and MK-801, and the difference in potency of the three blockers could be accounted for by differences in the reverse rate constants. Usually, the association rate of an open-channel blocker is markedly increased in the presence of agonist due to the removal of diffusion barriers by channel opening. However, the rate of dissociation of an open-channel blocker from the opened but blocked channel (the apparent off-rate) and the rate of leaving the closed and blocked channel (the leak rate from the trapped, unliganded state) have heretofore never been compared in a detailed manner.

Since the pseudo-first order association rate of a blocker with an open channel can be increased by simply increasing the concentration of the blocker, the main factor that determines the mode of antagonistic action resides in the relative off-rate of the blocker from the liganded-open but blocked state *versus* the unliganded-closed but blocked state (the latter representing the leak rate). For a potent and lipophilic open-channel blocker, such as MK-801 (Wong *et al.* 1986), the rate-limiting step of unbinding depends

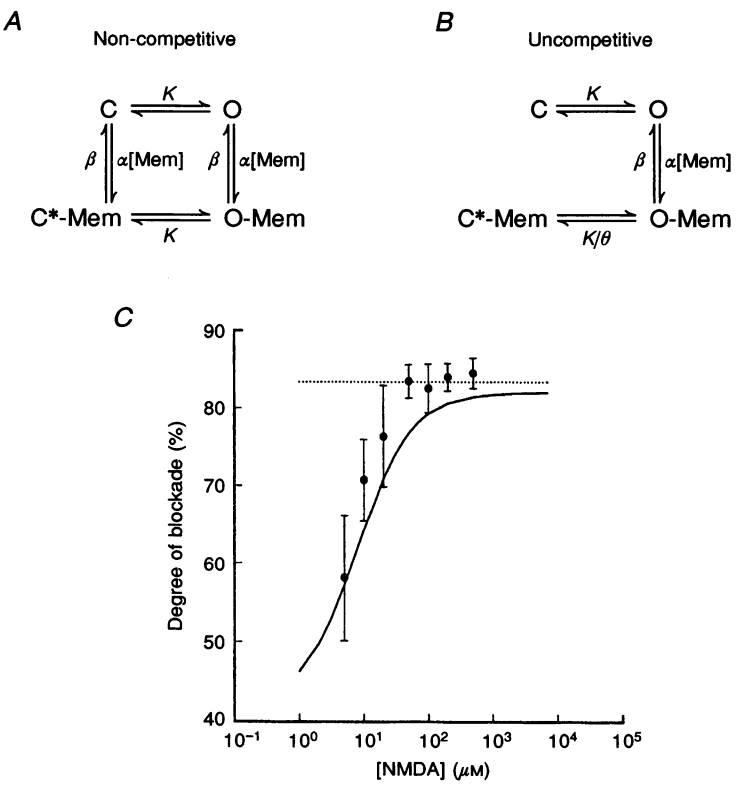

Figure 10. Difference in predicted degrees of blockade between non-competitive and uncompetitive antagonist action of memantine

A, scheme for non-competitive antagonism with C representing the closed channel; O, the open channel; C*-Mem, the blocked and closed channel; O-Mem, the open but blocked channel; α, the microscopic on-rate; β, the microscopic off-rate; [Mem], the concentration of the blocker; and K, the equilibrium constant for opening from the closed state, derived from P_o. The affinity of the blocker for the closed and open channel is the same. The open probability of the unblocked channel is the same as that of the blocked channel. *B*, scheme for uncompetitive antagonism. K/θ ($\theta = 0{\cdot}146$) is the equilibrium constant for opening from the C*-Mem state, and the rest of the symbols have the same meaning as in *A*. The blocker does not bind to the closed channel in this protocol. *C*, computer-simulated degree of blockade for non-competitive (dotted line) and uncompetitive (continuous curve) antagonism with the models and parameters indicated in *A* and *B*. Abscissa represents a logarithmic scale. The inhibition equilibrium constant (K_i) for the blocker is assumed to be 1·2 μM and [Mem] is 6 μM. The empirical data points were very close to those predicted theoretically for pure uncompetitive antagonism.

mainly on the nature of the blocker–channel complex and not on the diffusion pathway, which is either in the ionic solution or in the lipid bilayer. In other words, if the off-rate from the open but blocked channel is very slow, as in the case of MK-801, then the off-rate approaches the rate of leaving the closed and blocked channel via a hydrophobic pathway, which resembles non-competitive antagonism. From the kinetic data presented by Huettner & Bean (1988), MK-801 leaves the NMDA-gated channel with a mean τ of 90 min at −70 mV in the presence of NMDA, and recovers only ~10% after 20–30 min of washout in control solution without NMDA. From eqn (12), these data predict a leak τ of 190–285 min from the closed channel for MK-801. This leak rate is only 2- to 3-fold slower than the dissociation rate from the opened channel. The effect of blocker leaking out of the trapped state in this fashion would be to negate the stabilization of the open conformation of the blocked channel initiated by the binding of the blocker. As a result, the mode of antagonist action of MK-801 would have a significant component of non-competitive inhibition (Fig. 10*A*). In contrast, using the experimental protocol of Fig. 7*A* and eqn (12), the leak-rate constant for memantine was obtained from the percentage of recovery during exposure to control solution (without NMDA or memantine). This value was found to be less than 2% of the off-rate constant of memantine in the presence of 200 μM NMDA. The resulting uncompetitive nature of memantine (i.e. its close adherence to the theoretical continuous line in Fig. 10*C*), suggests that it will perform better therapeutically because it will display an increasing degree of blockade with increasing concentrations of agonist. Additional evidence for this kinetic hypothesis comes from an analysis of the action of the anaesthetic ketamine on NMDA-gated channels. Ketamine displays faster off-rate kinetics than most MK-801-like drugs, but is still slower than memantine (MacDonald *et al.* 1991); ketamine also has fewer clinical

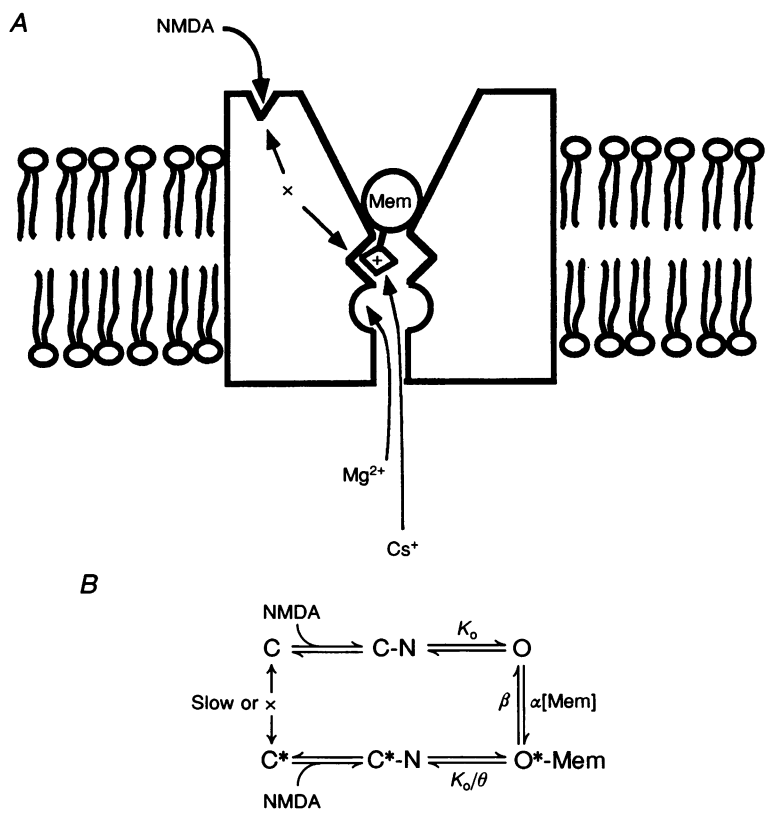

Figure 11. Model of memantine action of uncompetitive antagonism

A, schematic model of memantine antagonism. Memantine binds inside the channel pore and does not interact with the NMDA binding site. At physiological pH, the amine group on memantine is positively charged (NH_3^+; represented by ⊕ in the figure) and binds in the channel. The × between the NMDA and memantine binding sites indicates that the affinity for agonist is not affected by the presence of this antagonist. Internal permeant Cs^+ can compete with the externally applied memantine for binding, and memantine binding interacts with a Mg^{2+} binding site. *B*, final uncompetitive scheme for memantine inhibition. Memantine action requires prior activation of the channel and binds to the channel as a bimolecular process. Memantine rarely interacts with the closed channel but can be trapped within the channel when agonist is suddenly washed out. The gating process of the NMDA receptor-operated channel is faster than the kinetics of memantine action, and memantine binding stabilizes the open conformation of the blocked channel.

side-effects than MK-801 (Olney, Labruryere & Price, 1989), but more than memantine – in fact, the anaesthetic quality of ketamine may be due to its relatively prolonged blockade of NMDA-gated channels compared with memantine. Based on these observations, a therapeutically useful uncompetitive antagonist of the NMDA-gated channel should have a relatively faster off-rate from the open but blocked channel than its leak rate from the closed and blocked channel. However, this off-rate should not be as fast as the off-rate of Mg^{2+} which appears to be too fast to efficiently block overstimulation of NMDA receptor-operated channels activated by high levels of glutamate (Lipton, 1993).

Our fifth conclusion is that the memantine blocking site is most likely to be inside the channel pore, based upon an analysis of its voltage-dependent action. In general, the voltage dependence of open-channel blockade could arise from any of the following scenarios: (i) a binding site for the blocker inside the channel pore and within the membrane's potential field, which will therefore sense the voltage drop across the membrane (Woodhull, 1973; Vergara & Latorre, 1983); (ii) a binding site at the extracellular mouth of the channel, in which case the voltage-dependent binding of permeant cations from inside the cell would accelerate the off-rate of the blocker, thus conferring upon the blocker a voltage-dependent characteristic of antagonism (MacKinnon & Miller, 1988); (iii) voltage-dependent changes in open probability of the channel, which confer voltage dependence to the association rate of the antagonist and thus voltage dependence to the mechanism of antagonism (Anderson *et al.* 1988). After removal of internal permeant Cs^+, the calculated K_i of memantine is still voltage dependent, and this voltage dependence predicts a site of memantine binding that senses 52·6% of the transmembrane field from the outside (Fig. 9*A*). Most interestingly, at high millimolar concentrations, internal permeant Cs^+ actually competes with memantine binding and reduces its association rate while having no effect on the voltage dependence of the drug's dissociation rate. These observations strongly support the supposition that the memantine blocking site is within the permeation pathway of the channel pore, and that this site can apparently be accessed by internal permeant ions.

Additionally, the measured macroscopic unblocking rate (k_{off}) of memantine, equal to $\beta P_o'$, exhibited a very strong voltage dependence (Table 1 and Fig. 9*A*). However, this value was not corrected for the possible influence of voltage on the open probability of the blocked channel (P_o'). Since the voltage dependence of P_o' is not directly observable, the true voltage dependence of the microscopic off-rate (β) could be estimated only by assuming that the voltage dependence of P_o' is similar to the voltage dependence of P_o. This is a reasonable assumption because the binding of memantine stabilizes the open conformation of the blocked channel and does not affect the intrinsic process of NMDA receptor activation. Since nP_o is relatively stable between −60 and −20 mV (Nowak & Wright, 1992), the influence of P_o' on the voltage dependence of k_{off} would be minimal between −60 and −20 mV. Measuring the voltage dependence of k_{off} revealed that this rate constant increases with depolarization between −60 and −20 mV (Fig. 9*A*). Thus, k_{off} appears to be voltage dependent even after correction for P_o'. In the same voltage range, the macroscopic blocking rate of memantine (k_{on}) also displays a significant voltage dependence, which cannot be totally accounted for by the presence of internal permanent Cs^+ because the currents were predominantly inward.

Neither can the influence of external permeant cations account for the voltage dependence of the on- and off-rates of memantine blockade. If external permeant cations competed with memantine binding, the competition would be stronger at negative potentials and weaker at positive potentials. This would result in a slower on-rate of memantine at hyperpolarized potentials and a faster on-rate at depolarized potentials. However, the observed voltage dependence of the on-rate of memantine (Fig. 9*B*) was slower at positive potentials and faster at negative potentials. Correction for the effect of competition by external cations would only make the on-rate more voltage dependent instead of less voltage dependent. Therefore, the on-rate of memantine action must be voltage dependent, and this is consistent with a binding site for memantine that is inside the pore. In addition, since memantine only blocks the NMDA-gated channel from the outside and can only escape to the outside when the channel is re-activated, external cations could only affect k_{off} by a 'lock-in' phenomenon in a multi-ion pore (Neyton & Miller, 1988). However, even if a 'lock-in' phenomenon exists, memantine must bind inside the pore within the permeation pathway of the channel.

In conclusion, memantine antagonizes 200 μM NMDA-induced responses by a mechanism of open-channel block with a K_i of ~1 μM at a holding potential of −60 mV. The present experiments demonstrate for the first time for this NMDA open-channel blocker that (i) the antagonist can be trapped in the closed and blocked channel; (ii) the much faster off rate of memantine from the open but blocked channel than leak rate from the trapped state is a principal determinant of the drug's uncompetitive mode of action; (iii) the association rate of memantine is still voltage dependent even after correction for the influence of open probability (P_o); and (iv) internal permeant cations can compete with externally applied memantine. Considering the voltage dependence of K_i and k_{off}, the memantine binding site must lie within the channel pore at an electrical distance of approximately 30–50% of the transmembrane field from the outside. Combining this evidence, a final schematic diagram for the uncompetitive mode of memantine action is presented in Fig. 11. The diagram illustrates that at pH 7·2 the bridgehead amine group of memantine is positively charged ($-NH_3^+$) and competes with Cs^+ for a site within the channel.

AIZENMAN, E., FROSCH, M. P. & LIPTON, S. A. (1988). Responses mediated by excitatory amino acid receptors in solitary retinal ganglion cells from rat. *Journal of Physiology* **396**, 75–91.

ANDERSON, C. S., MACKINNON, R., SMITH, C. & MILLER, C. (1988). Charybdotoxin block of single Ca^{2+}-activated K^+ channels. *Journal of General Physiology* **91**, 317–333.

BORMANN, J. (1989). Memantine is a potent blocker of *N*-methyl-D-aspartate (NMDA) receptor channels. *European Journal of Pharmacology* **166**, 591–592.

CHEN, H.-S. V. (1992). Memantine: Open-channel block of *N*-methyl-D-aspartate (NMDA) elicited responses. PhD Thesis, Harvard University, Cambridge, USA.

CHEN, H.-S. V., PELLEGRINI, J. W., AGGARWAL, S. K., LEI, S. Z., WARACH, S., JENSEN, F. E. & LIPTON, S. A. (1992). Open-channel block of *N*-methyl-D-aspartate (NMDA) responses by memantine: Therapeutic advantage against NMDA receptor-mediated neurotoxicity. *Journal of Neuroscience* **12**, 4427–4436.

CHOI, D. W. (1988). Glutamate neurotoxicity and diseases of the nervous system. *Neuron* **1**, 623–634.

HAMILL, O. P., MARTY, A., NEHER, E., SAKMANN, B. & SIGWORTH, F. J. (1981). Improved patch-clamp techniques for high resolution current recordings from cells and cell free membrane patches. *Pflügers Archiv* **391**, 85–100.

HILLE, B. (1984). *Ionic Channels of Excitable Membranes.* Sinauer Associates, Sunderland, MA, USA.

HOWE, J. R., CULL-CANDY, S. G. & COLQUHOUN, D. (1991). Current through single glutamate receptor channels in outside-out patches from rat cerebellar granule cells. *Journal of Physiology* **432**, 143–202.

HUETTNER, J. E. & BEAN, B. P. (1988). Block of *N*-methyl-D-aspartate-activated current by the anticonvulsant MK-801: Selective binding to open channels. *Proceedings of the National Academy of Sciences of the USA* **85**, 1307–1311.

KARSCHIN, A., AIZENMAN, E. & LIPTON, S. A. (1988). The interaction of agonists and noncompetitive antagonists at the excitatory amino acid receptors in rat retinal ganglion cells *in vitro*. *Journal of Neuroscience* **8**, 2895–2906.

KARSCHIN, A. & LIPTON, S. A. (1989). Calcium channels in solitary retinal ganglion cells from post-natal rat. *Journal of Physiology* **418**, 379–396.

KEMP, J. A., FOSTER, A. C. & WONG, E. H. F. (1987). Non-competitive antagonists of excitatory amino acid receptors. *Trends in Neurosciences* **10**, 294–298.

KORNHUBER, J., BORMANN, J., RETZ, W., HÜBERS, M. & RIEDERER, P. (1989). Memantine displaces [^{3}H]MK-801 at therapeutic concentrations in postmortem human frontal cortex. *European Journal of Pharmacology* **166**, 589–590.

LEIFER, D., LIPTON, S. A., BARNSTABLE, C. J. & MASLAND, R. H. (1984). Monoclonal antibody to Thy-1 enhances regeneration of processes by rat retinal ganglion cells in culture. *Science* **224**, 303–306.

LIPTON, S. A. (1993). Prospects for clinically tolerated NMDA antagonists: open-channel blockers and alternative redox states of nitric oxide. *Trends in Neurosciences* **16**, 527–532.

LIPTON, S. A. & GENDELMAN, H. E. (1995). Dementia associated with the acquired immunodeficiency syndrome. *New England Journal of Medicine* **332**, 934–940.

LIPTON, S. A. & ROSENBERG, P. A. (1994). Excitatory amino acids as a final common pathway for neurologic disorders. *New England Journal of Medicine* **330**, 613–622.

LIPTON, S. A. & TAUCK, D. L. (1987). Voltage-dependent conductances of solitary ganglion cells dissociated from the rat retina. *Journal of Physiology* **385**, 361–391.

MACDONALD, J. F., BARTLETT, M. C., MODY, I., PAHAPILL, P., REYNOLDS, J. N., SALTER, M. W., SCHNEIDERMAN, J. H. & PENNEFATHER, P. S. (1991). Actions of ketamine, phencyclidine and MK-801 on NMDA receptor currents in cultured mouse hippocampal neurones. *Journal of Physiology* **432**, 483–508.

MACDONALD, J. F., MODY, I. & SALTER, M. W. (1989). Regulation of *N*-methyl-D-aspartate receptors revealed by intracellular dialysis of murine neurons in culture. *Journal of Physiology* **414**, 17–34.

MACKINNON, R. & MILLER, C. (1988). Mechanism of charybdotoxin block of the high-conductance, Ca^{2+}-activated K^+ channel. *Journal of General Physiology* **91**, 335–349.

MAYER, M. L., VYKLICKY, L. JR & CLEMENTS, J. (1989). Regulation of NMDA receptor desensitization in mouse hippocampal neurons by glycine. *Nature* **338**, 425–427.

MAYER, M. L., WESTBROOK, G. L. & GUTHRIE, P. B. (1984). Voltage-dependent block by Mg^{2+} of NMDA responses in spinal cord neurones. *Nature* **399**, 261–263.

MEGURO, H., MORI, H., ARAKI, K., KUSHIYA, E., KUTSUWADA, T., YAMAZAKI, M., KUMANISHI, T., ARAKAWA, M., SAKIMURA, K. & MISHINA, M. (1992). Functional characterization of a heteromeric NMDA receptor channel expressed from cloned cDNAs. *Nature* **357**, 70–74.

MELDRUM, B. S., TURSKI, L., SCHWARZ, M., CZUCZWAR, S. J. & SONTAG, K.-H. (1986). Anticonvulsant action of 1,3-dimethyl-5-amino-adamantane. *Naunyn–Schmiedeberg's Archives of Pharmacology* **332**, 93–97.

MELDRUM, B. & GARTHWAITE, J. (1990). Excitatory amino acid neurotoxicity and neurodegenerative disease. *Trends in Pharmacological Sciences* **11**, 379–387.

MILLER, C. (1987). Trapping single ions in single ion channels. *Biophysical Journal* **52**, 123–126.

MILLER, C., LATORRE, R. & REISIN, I. (1987). Coupling of voltage-dependent gating and Ba^{2+} block in the high-conductance, Ca^{2+}-activated K^+ channel. *Journal of General Physiology* **90**, 427–449.

MONYER, H., SPRENGEL, R., SCHOEPFER, R., HERB, A., HIGUCHI, M., LOMELI, H., BURNASHEV, N., SAKMANN, B. & SEEBURG, P. H. (1992). Heteromeric NMDA receptors: molecular and functional distinction of subtypes. *Science* **256**, 1217–1221.

NOWAK, L., BREGESTOVSKI, P., ASCHER, P., HERBERT, A. & PROCHIANTZ, A. (1984). Magnesium gates glutamate-activated channels in mouse central neurons. *Nature* **307**, 462–465.

NOWAK, L. M. & WRIGHT, J. M. (1992). Slow voltage-dependent changes in channel open-state probability underlie hysteresis of NMDA responses in Mg^{2+}-free solutions. *Neuron* **8**, 181–187.

NEYTON, J. & MILLER, C. (1988). Potassium blocks barium permeation through a calcium-activated potassium channel. *Journal of General Physiology* **92**, 549–567.

OLNEY, J. W., LABRURYERE, J. & PRICE, M. T. (1989). Pathological changes induced in cerebrocortical neurons by phencyclidine and related drugs. *Science* **244**, 1360–1362.

PENNEFATHER, P. & QUASTEL, D. M. (1982). Modification of dose–response curves by effector blockade and uncompetitive antagonism. *Molecular Pharmacology* **22**, 369–380.

ROGAWSKI, M. A. (1993). Therapeutic potential of excitatory amino acid antagonists: channel blockers and 2,3-benzodiazepines. *Trends in Pharmacological Sciences* **14**, 325–331.

ROTHMAN, S. M. & OLNEY J. W. (1987). Excitotoxicity and the NMDA receptor. *Trends in Neurosciences* **10**, 299–302.

SCHNEIDER, E., FISCHER, P.-A., CLEMENS, R., BALZEREIT, F., FÜNFGELD, E.-W. & HAASE, H.-J. (1984). Wirkungen oraler Memantin-gaben auf die Parkinson-symptomatik. *Deutsche Medizinische Wochenzeitschrift* **109**, 987–990.

SCHWAB, R. S., ENGLAND, A. C., POSKANZER, P. C. & YOUNG, R. Y. (1969). Amantadine in the treatment of Parkinson's disease. *Journal of the American Medical Association* **208**, 1168–1170.

SERNAGOR, E., KUHN, D., VYKLICKY, L. JR & MAYER, M. L. (1989). Open channel block of NMDA receptor responses evoked by tricyclic antidepressants. *Neuron* **2**, 1221–1227.

STARMER, C. F. PACKER, D. L. & GRANT, A. O. (1987). Ligand binding to transiently accessible sites: mechanisms for varying apparent binding rates. *Journal of Theoretical Biology* **124**, 335–341.

STARMER, C. F., YEH, J. Z. & TANGUY, J. (1986). A quantitative description of QX222 blockade on sodium channels in squid axons. *Biophysical Journal* **49**, 913–920.

STERN, P., BÉHÉ, P., SCHOEPFER, R. & COLQUHOUN, D. (1992). Single channel conductances of NMDA receptors expressed from cloned cDNAs: comparison with native receptors. *Proceedings of the Royal Society* B **250**, 271–277.

TAUCK, D. L., FROSCH, M. P. & LIPTON, S. A. (1988). Characterization of GABA- and glycine-induced currents of solitary rodent retinal ganglion cells in culture. *Neuroscience* **27**, 193–203.

TOMINACK, R. L. & HAYDEN, F. G. (1987). Rimantadine hydrochloride and amantadine hydrochloride use in influenza A virus infections. *Infectious Disease Clinics of North America* **1**, 459–478.

VERGARA, C. & LATORRE, R. (1983). Kinetics of Ca^{2+}-activated K^+ channels from rabbit muscle incorporated into planar bilayers. *Journal of General Physiology* **82**, 543–568.

VIGNON, J., VINCENT, J.-P., BIDARD, J.-N., KAMENKA, J.-M., GENESTE, P., MONIER, S. & LAZDUNSKI, M. (1982). Biochemical properties of the brain phencyclidine receptor. *European Journal of Pharmacology* **81**, 531–542.

VYKLICKY, L. JR, BENVENISTE, M. & MAYER, M. L. (1990). Modulation of *N*-methyl-D-aspartic acid receptor desensitization by glycine in mouse cultured hippocampal neurones. *Journal of Physiology* **428**, 313–331.

WANG, G. K. (1990). Binding affinity and stereoselectivity of local anesthetics in single batrachotoxin-activated Na^+ channels. *Journal of General Physiology* **96**, 1105–1127.

WONG, E. H. F. & KEMP, J. A. (1991). Sites for antagonism on the *N*-methyl-D-aspartate receptor channel complex. *Annual Review of Pharmacology and Toxicology* **31**, 401–425.

WONG, E. H. F., KEMP, J. A., PRIESTLEY, T., KNIGHT, A. R., WOODRUFF, G. N. & IVERSEN, L. L. (1986). The anticonvulsant MK-801 is a potent *N*-methyl-D-aspartate antagonist. *Proceedings of the National Academy of Sciences of the USA* **83**, 7104–7108.

WOODHULL, A. M. (1973). Ionic blockage of sodium channels in nerve. *Journal of General Physiology* **61**, 687–708.

WRIGHT, J. M., KLINE, P. A. & NOWAK, L. M. (1991). Multiple effects of tetraethylammonium on *N*-methyl-D-aspartate receptor-channels in mouse brain neurons in cell culture. *Journal of Physiology* **439**, 579–604.

Acknowledgements

We are grateful to Dr J. Bormann for initially suggesting the use of memantine as an NMDA antagonist to us and to Dr G. Quack for the kind gift of memantine (Merz and Co., Frankfurt, Germany). We also thank Drs Gary Strichartz, Bruce Bean, Linda Nowak and the late Peter Hess for their critical review and comments on this work. This work was supported in part by NIH grants R01 EY05477, R01 EY09024, and P01 HD29587 to Dr S. A. Lipton.

Author's email address

S. A. Lipton: Lipton_s@a1.tch.harvard.edu

Received 11 October 1996; accepted 13 November 1996.